Paper 32

Numerical and Experimental Study on Flow and Diffusion Field in Room.

Shuzo Murakami , Shinsuke Kato

Institute of Industrial Science
University of Tokyo
22-1 Roppongi 7-chome, Minato-ku Tokyo 106
Japan

SYNOPSIS

Turbulent flow fields of velocity and diffusion in several types of mechanically ventilated rooms are precisely analyzed both by model experiment and by numerical simulation based on the $k-\varepsilon$ two-equation turbulence model. The detailed analyses of contaminant diffusion by simulation make it possible to comprehend clearly the structures of velocity and diffusion fields in rooms.

The flow fields in such rooms, as analyzed here, are mainly characterized by the inflow jet and the rising streams around it. The combination of one jet and rising streams forms a 'flow unit.' The total velocity field and the resulting diffusion field of contaminant in a room are well modeled as serial combinations of these 'flow units.'

Room air distribution is greatly affected by the arrangement of supply openings and, possibly, exhaust openings. The influence of those arrangements on the flow fields is studied. When the number of supply openings is decreased, the flow units corresponding to the eliminated supply openings vanish and the remaining flow units expand. A change in arrangement or in the number of exhaust openings hardly affects the entire flow field; however, such changes often have a large influence on the contaminant diffusion field.

Apparatus placed in a room has a great influence on the flow field. The air flow distribution and the contaminant diffusion field in the room with flow obstacles in various arrangements are also analyzed. On the whole, the influence of flow obstacles on the entire flow field is limited to a certain degree, however, the influence on the 'flow unit' is significant.

NOMENCLATURE

C_μ, C_1, C_2	= empirical constants in the $k-\varepsilon$ turbulence model (cf. Table 2)
C	= mean contaminant concentration
C_0	= representative concentration defined by that of exhaust opening
E	= empirical constant in log law, 9.0 in case of smooth wall
h	= interval of finite difference
h_1	= length from the solid wall surface to the center of the near wall fluid cell
k	= turbulence kinetic energy
1	= length scale of turbulence
L_0	= representative length defined by width of supply opening
P	= mean pressure
q	= contaminant generation rate
Q	= air exchange volume
SVE	= scale for ventilation efficiency

    SVE1, spatial average concentration

    SVE2, mean radius of diffusion

    SVE3, concentration in case of uniform contaminant generation throughout the room

U_i, U_j	= components of mean velocity vector
U_0	= representative velocity defined by inflow jet velocity
ε	= turbulence dissipation rate

κ = von Karman constant, 0.4
ρ = fluid density
ν = molecular kinematic viscosity
ν_t = eddy kinematic viscosity
$\sigma_1, \sigma_2, \sigma_3$ = turbulence Prandtl/Schmidt number of k, ε, C (cf. Table 2)

1. INTRODUCTION

The airflow pattern in a room is mainly determined by the shape of the room and the number of supply openings. Therefore, in order to accurately design the airflow for such a room, one should analyze each room independently. However, it is also well-known that the flow fields of such rooms share many common characteristics, especially when the supply openings are set on the ceiling. In this study, the flow fields and resulting diffusion fields of contaminant in rooms, where supply openings are located on the ceiling, are precisely analyzed.

The distribution of contaminant diffusion is a very useful means by which to comprehend the diffusion field. On the other hand, the diffusion field alone cannot give effective information for evaluating ventilation efficiency because, when given two patterns of contaminant diffusion, it is often difficult to judge which one is better. For this purpose, we need a simple index that can express the characteristics of the diffusion pattern as a quantitative value. Kato and Murakami (1988) proposed the new concept of ventilation efficiency for the diffusion fields of contaminant and presented a method by which to estimate the different distributions of contaminant concentration as a whole and to evaluate the difference of ventilation efficiency. We will here briefly summarize the new concept of ventilation efficiency and apply it to the diffusion fields in the rooms under discussion.

As stated above, the airflow pattern in a room is mainly determined by the shape of the room and by the number of supply openings. In this study, the influence of the arrangement and number of supply and exhaust openings on the flow and diffusion fields in rooms and the effects of the flow obstacle are analyzed from the viewpoint of flow structure and the ventilation efficiency.

Numerical simulation of turbulent air flow allows us to analyze the flow and diffusion fields in a room precisely (Murakami et al. 1987). It is confirmed that the correspondence between experiment and numerical simulation is fairly good for both velocity vectors and contaminant concentration. Analysis by numerical method is very powerful in parametric study is. The influences of various flow conditions on the flow and diffusion fields are analyzed parametrically here. Thus, in this paper, flow fields and contaminant diffusion fields are examined mainly by means of numerical simulation.

MODEL ROOMS ANALYZED

Eight types of rooms are used for analysis in this study. In table 1, the specifications of these rooms are presented. These rooms may be regarded as the models of conventional flow type clean rooms. Length and velocity scales are non-dimentionalized by dividing by the representative values, the width of supply opening L_0, and the supply air velocity V_0, respectively. Figure 1 shows the plans and sections of these 8 types. The source points of contaminant are located under the supply opening, near the wall, and at the center of the room, respectively. Their height from the floor is set equally at 1.25 in dimensionless value. Another source point of contaminant is located in front of the exhaust opening, where its height from the floor is 0.5. Since the contaminant in this study is assumed to be of passive scalar quantity, and thus of no effect on momentum equations, its transportation or diffusion is fully controlled by the air flow. Flow fields and resulting diffusion fields are assumed to be in steady states. The contaminant generation rate is also assumed to be constant.

Table 1. Specifications of model rooms used

Types of Model Clean Room	Dimension of Plan (*1)	Height of Ceiling (*1)	Number of Supply openings	Number of Exhaust openings	Supply Air Velocity (*2)	Remarks
TYPE 1	5 X 5	4.5	1	4	1.0	basic type:the smallest room
TYPE 2	8 X 8	4.5	4	4	1.0	basic type
TYPE 3	8 X 8	4.5	4	4	1.0	2 exhaust openings are closed
TYPE 4	11X11	4.5	9	4	1.0	basic type:the largest room
TYPE 5	11X11	4.5	6	4	1.0	3 supply openings are closed
TYPE 6	11X11	4.5	5	4	1.0	4 supply openings are closed
TYPE 7	11X11	4.5	4	4	1.0	5 supply openings are closed
TYPE 8	11X11	4.5	1	4	1.0	8 supply openings are closed

*1 : dimensionless value (divided by the width of supply opening L_0 (0.6m))
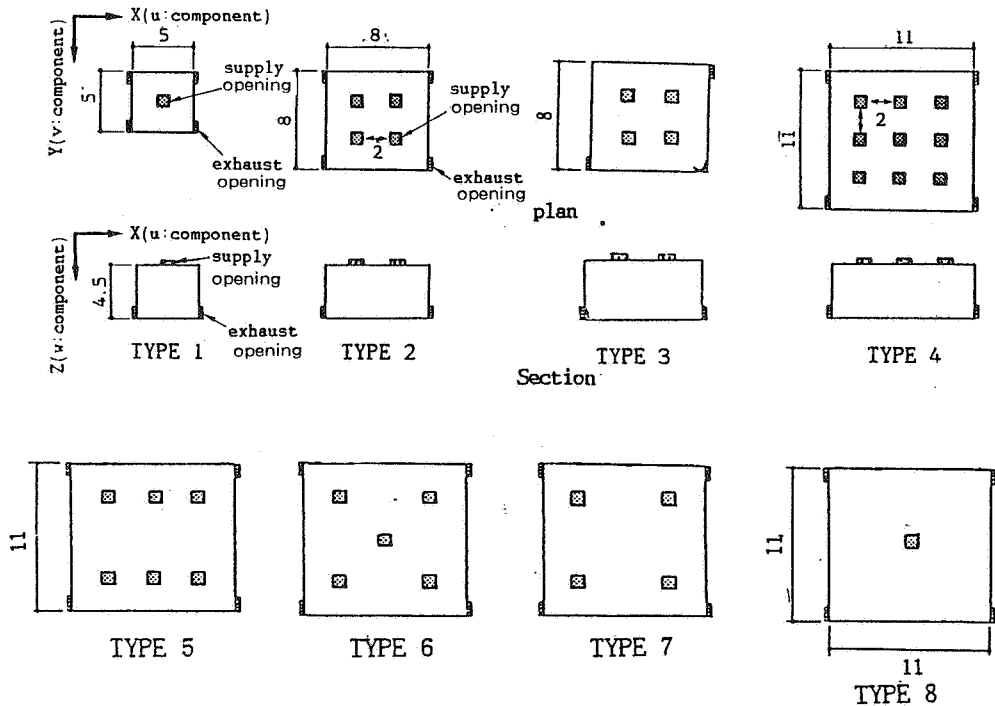*2 : dimensionless value (divided by the supply air velocity V_0 (1.0m/s))

Figure 1. Plans and sections of model rooms (Length scale in this figure is non-dimensionalized by the width of supply outlet Lo)

3. MODEL EXPERIMENTS

Model experiments were conducted using scale models. The representative length, the width of supply opening L_0, was set as 0.1 m in all room models. The velocity of the jet from supply opening U_0 was set at 6 m/s. The Reynolds number of the inflow jet $U_0 L_0 / \nu$ is 4.2×10^4.

Air velocity is measured by means of tandem type, parallel hot-wire anemometer, which can discern the vector components of turbulent flow (Murakami et al.1980).

The distribution of contaminant concentration is investigated by means of a tracer gas diffusion experiment. Since ethylene (C_2H_4), whose density is nearly the same as that of air, is used as the tracer, the buoyancy effect of the tracer can be disregarded. Its concentration is measured by means of F.I.D. gas chromatography.

Table 2. Two-Equation Model (Three-Dimensional)

$\frac{\partial U_i}{\partial X_i} = 0$	(1) Continuity equation
$\frac{\partial U_i}{\partial t} + \frac{\partial U_i U_j}{\partial X_j} = -\frac{\partial}{\partial X_i}\{\frac{P}{\rho} + \frac{2}{3}k\} + \frac{\partial}{\partial X_j}\{\nu_t(\frac{\partial U_i}{\partial X_j} + \frac{\partial U_j}{\partial X_i})\}$	(2) Momentum equation
$\frac{\partial k}{\partial t} + \frac{\partial k U_j}{\partial X_j} = \frac{\partial}{\partial X_j}\{\frac{\nu_t}{\sigma_1}\frac{\partial k}{\partial X_j}\} + \nu_t S - \varepsilon$	(3) Transport equation for k
$\frac{\partial \varepsilon}{\partial t} + \frac{\partial \varepsilon U_j}{\partial X_j} = \frac{\partial}{\partial X_j}\{\frac{\nu_t}{\sigma_2}\frac{\partial \varepsilon}{\partial X_j}\} + C_1\frac{\varepsilon}{k}\nu_t S - C_2\frac{\varepsilon^2}{k}$	(4) Transport equation for ε
$\nu_t = k^{1/2} l = \{C_\mu \frac{k^2}{\varepsilon}\}$	(5) Equation for deciding ν_t
$\frac{\partial C}{\partial t} + \frac{\partial C U_j}{\partial X_j} = \frac{\partial}{\partial X_j}\{\frac{\nu_t}{\sigma_3}\frac{\partial C}{\partial X_j}\}$	(6) Concentration equation

here $S = \{\frac{\partial U_i}{\partial X_j} + \frac{\partial U_j}{\partial X_i}\}\frac{\partial U_i}{\partial X_j}$, $\sigma_1 = 1.0$, $\sigma_2 = 1.3$, $\sigma_3 = 1.0$
$C_\mu = 0.09$, $C_1 = 1.44$, $C_2 = 1.92$

Table 3. Boundary Conditions for Numerical Simulation

(1) Supply Outlet : $U_t = 0.0$, $U_n = U_{out}$, $k = 0.005$, $l = 0.33$, $C = 0.0$
boundary   suffix t: tangential component, n: normal component
               U_{out} : Supply opening velocity, $U_{out} = 1.0$

(2) Exhaust Inlet : $U_t = 0.0$, $U_n = U_{in}$, $\partial k/\partial Z = 0.0$, $\partial \varepsilon/\partial Z = 0.0$, $\partial C/\partial Z = 0.0$
boundary U_{in}: Exhaust opening velocity, $U_{in} = 2.25$ in case of TYPE 4

(3) Wall boundary : $\partial U/\partial Z_{Z=0} = m U_t{}_{Z=h}/h$, $U_n = 0.0$, $\partial k/\partial Z = 0.0$, $\partial C/\partial Z = 0.0$

ε term in k equation :

$\varepsilon_{Z=h} = [C_\mu k_{Z=h}^{3/2}]/[C_\mu^{1/4}\kappa h] \cdot \ln(E h(C_\mu^{1/2} k)^{1/2}/\nu)$

ε equation :

$\varepsilon_{Z=h} = [C_\mu k_{Z=h}^{3/2}]/[C_\mu^{1/4}\kappa h]$

h : Length from the wall surface to the center of the adjacent cell
m : 1/7, Power law of profile $U_t \propto Z^m$ is assumed here.
E : 9.0, a function of the wall roughness (for a smooth wall)
ν : 1/Re, Kinematic viscosity
κ : 0.4, von Karman constant

(4) Finite   : Time marching : Adams Bashforth Scheme (second order)
    difference
    Scheme   Convective   : Quick Scheme (second order)
               terms of Ui,
               k, ε, and C

(Values are expressed in non-dimensional form)

4. NUMERICAL SIMULATION METHOD

Model equations (3-D k- ε two-equation turbulence model) are given in Table 2. The boundary conditions are tabulated in Table 3. Various types of boundary conditions at the solid wall have been devised in various problems of engineering applications of the numerical method. Some boundary conditions were derived using the concept of log-law (Launder et al.1974; Chieng et al.1980; Rodi 1984). The solid wall boundary condition derived from the power law of velocity profile is used (authors cf. Table 3). The latter is very simple and has given successful results (Murakami et al.1987; Murakami et al.1988).The difference in the simulation results between these log-law types and the power law type has been examined and confirmed to be negligibly small(Kato et al.1988b; Nagano et al.1988). In this context,the solid wall boundary condition derived from the power law of velocity profile is used here.

The flow fields in rooms divided into the mesh systems shown in Figure 2 are solved by the finite difference method. The numerical simulation method follows that given in Murakami et al.(1987). After the room flow fields are obtained, the contaminant diffusion fields are calculated using such flow field properties as the distribution of velocity vectors and eddy viscosity. The simulated flow fields are not entirely steady and symmetrical due to numerical instability. However, asymmetry of flow fields is very slight and can be disregarded. The calculated contaminant diffusion fields are thus also slightly asymmetric in accord with the flow fields.
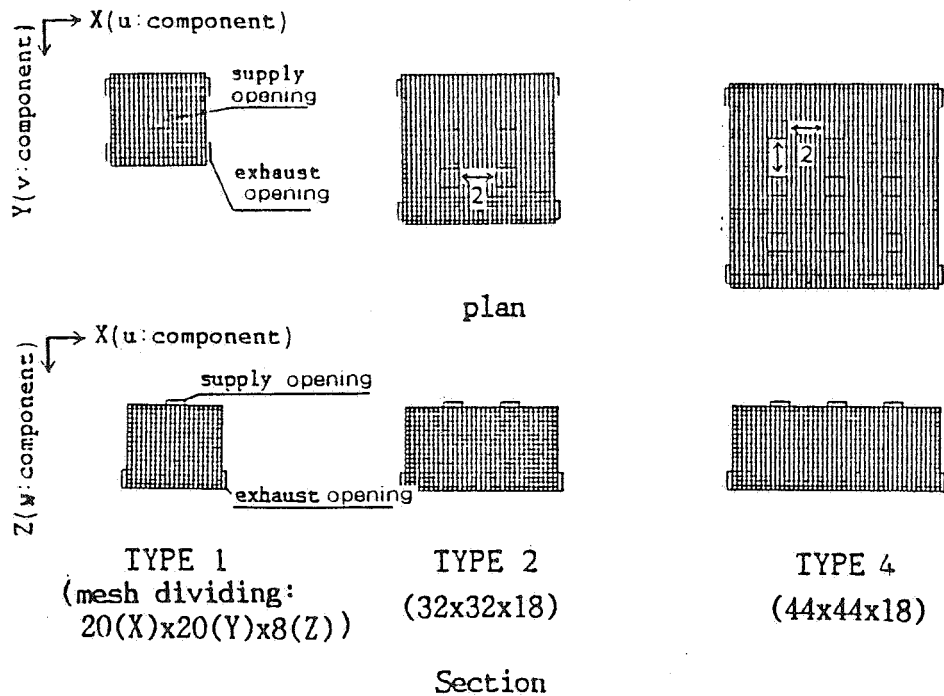

plan

TYPE 1
(mesh dividing:
20(X)x20(Y)x8(Z))

TYPE 2
(32x32x18)

TYPE 4
(44x44x18)

Section

Figure 2. Mesh systems

5. EXPRESSION METHODS OF CONTAMINANT DIFFUSION FIELD AND DEFINITION OF SVE1,2,3

In this study, contaminant diffusion fields are expressed by four methods:

1. Distribution of contaminant concentration in case of point source: this distribution allows intuitive comprehension of the contaminant diffusion field in a room.

2. Spatial average concentration: the first Scale of Ventilation Efficiency (SVE1). This value is proportional to the average time the
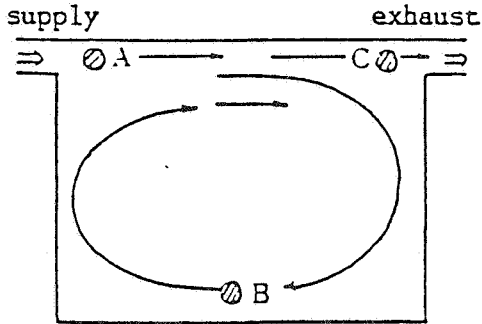
- Contaminant source point A
  mean radius of diffusion (SEV2) : large
  spatial average concentration (SEV1)
  $\approx$ concentration in exhaust
- Contaminant source point B
  mean radius of diffusion : large
  spatial average concentration
  $>$ concentration in exhaust
- Contaminant source point C
  mean radius of diffusion : very small
  spatial average concentration
  $\ll$ concentration in exhaust

Figure 3. Change of diffusion field according to the change of source position
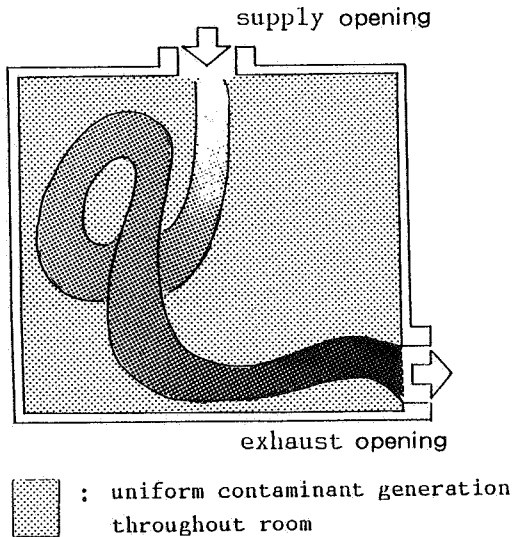
- SEV3 is defined as the value of concentration at each point.
- It is an index of the travelling time for an air mass blown from supply openings to arrive at each point.

: uniform contaminant generation throughout room

Figure 4. SVE3 : Diffusion field in case of contaminant generated uniformly throughout the room

contaminant is present in the room and indicates how quickly the contaminant generated in the room is exhausted by the flow field. This condition may be easily explained as follows. When the generated contaminant takes more time to be convected to the exhaust opening, it is certain that there exists more contaminant within the room in spite of the constant generation and constant exhaust of contaminant. Figure 3 shows the change of the value of SVE1 according to position of the source. If the contaminants are generated near the exhaust, at point C, the contaminants are smoothly exhausted and the value of SVE1 is expected surely to be very small. However, if the contaminants are generated within the recirculating flow, at point B, the contaminants are likely to stay longer in the room and the value of SVE1 will increase.

3. Mean radius of diffusion: the second Scale of Ventilation Efficiency (SVE2). This value represents the average spatial diffusion. Figure 3 shows the change of the value of SVE2 according to position of the source. If the contaminants are generated near exhaust, at point C, the contaminants are exhausted without diffusion. In this case, the value of SVE2 is expected surely to be very small. However, if the contaminants are generated at the supply opening, at point A, the contaminants spread and diffuse throughout the room. The value of SVE2 is expected to be the largest.

4. Concentration in case of uniform contaminant generation throughout the room: the third Scale of Ventilation Efficiency (SVE3). At a given point in a room this value is proportional to the mean travelling time of the supply air to that point. High value of this scale indicates a high possibility of air contamination, because the air mass must have travelled a long way from the supply opening to that point. This situation is illustrated in Figure 4.

The details of these scales are described by Kato et al.(1988a)

6. DIMENSIONLESS STUDY OF CONCENTRATION (MODELS 1 AND 2)

In this study, concentration is made dimensionless by dividing by representative value of C_0, the mean contaminant concentration averaged over all exhaust openings. The value of C_0 is necessarily equal to the ratio of the contaminant generation rate to the supply air volume rate. The value of C_0 may be changed according to the room type in which the ratio of the generation rate to the supply air volume rate may be changed. Thus, two kinds (Models 1 and 2) of dimensionless concentration are used. Model 1 is defined as the concentration non-dimensionalized by the individual C_0 of the each room type. In Model 2, the value of C_0 of a basic type is commonly used for non-dimensionalization. Both of Model 1 and Model 2 are important for the various analysis of diffusion field.

The values of SVE1 is generally calculated using the non-dimensional data of Model 1, given by the numerical simulation, since this scale expresses the individual properties of each diffusion field.

However Model 1 is not convenient for comparing the different diffusion fields because the representative value of C_0 is not common. When we want to compare two dimensionless concentration distribution fields, the value of C_0 must be held in common. If the representative concentration used for non-dimensionalizing the concentration is identical, the two dimensionless

concentration fields can be compared directly. For this purpose, the value of C_0 for the basic type is often used as the common representative concentration. This dimensionless concentration is defined as Model 2.

7. CORRESPONDENCE BETWEEN EXPERIMENT AND SIMULATION

7.1 Flow Field

   As is shown in Figure 5 (a) and (c), Figure 7 (a) and (c),and also Figure 15(a) and Figure 16(a), the results of the simulation of the flow field correspond well with those of the experiment. Figure 5(a) and (c) show a comparison of the simulated results with the experimental results for the distribution of the velocity vectors for Type 1 room. Figure 7 (a) and (c) show a comparison in the case of Type 2. Detailed comparisons are given in Murakami et al.(1988)
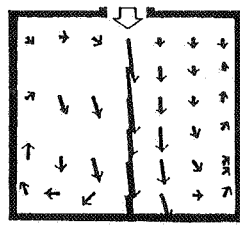

7.2 Diffusion Field

   As is shown in Figure 5 (b) and (d), Figure 7 (b) and (d), and Figure 15 (b) and Figure 17 (a), the results of the simulation of the contaminant diffusion field, correspond well to those of the experiment. Although the contour lines of concentration are not exactly the same, the main characteristics of the contaminant diffusion are well reproduced, that is, the shape of the high concentration region, the low concentration region under the supply outlet, and so on. However, the result of the simulation tends to be more diffusive than those obtained by the experiment, thus the values of the contaminant concentration tends to be smaller than those given by the experiments for areas where the concentration is high and to be larger for areas where the concentration is low.
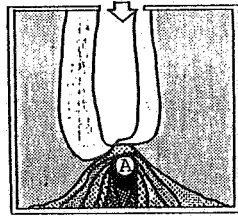

8 FLOW AND DIFFUSION FIELD FOR TYPE 1 (ONE SUPPLY OPENING, Figures 5,6)

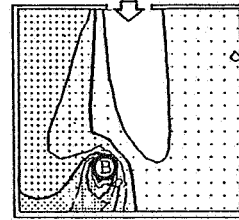8.1 In the Case of Contaminant Generated under Supply Opening

   The flow field is shown in Figure 5 (c) and (e). The jet from the supply opening attacks the floor and diverges toward the wall. The diverged streams reach the sidewalls and turn up toward the ceiling. The distribution of concentration in the case where the contaminant is generated in the supply jet is shown in Figure 5 (d) and (f). The contaminant source point is marked as A. The concentration is very high in the area between the source and floor. However; the value of the concentration is rather uniform throughout the room and is more than 0.5 (non-dimensional value), except for the area just beneath the supply opening where it is very clean (Figure 5 (d)). The spatial average concentration, SVE1, is 0.9 and the mean radius of diffusion, SVE2, is 2.8 (non-dimensionalized by L_0), which is 29% of the relevant length of the room, 8.4. The relevant length of the room is defined as the square root of the sum of the square of each of the three dimensions of the room.
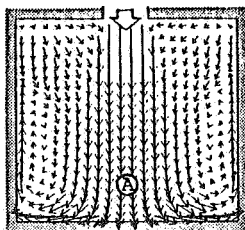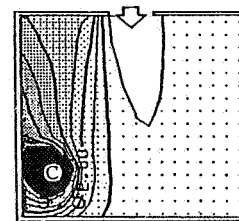
(a) velocity vectors (b) concentration : source A
    Experiment   Experiment

(a) source : B

(c) velocity vectors (d) concentration : source A
    Simulation   Simulation
    including supply opening(section)

(b) source : C

(e) velocity vectors (f) concentration : source A
    Simulation   Simulation
    including exhaust openings(plan)

(c) source : D
including supply opening (section)

5.0 4.0 3.0 2.0 1.0 0
Dimensionless concentration
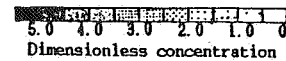
Illustrated plane
(Fig.5, 6)

Fig.5-(a)-(d)   O sources
Fig.6-(a)-(c)
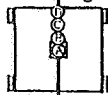
⊕ Fig.5-(e),(f)

(plan)   (section)

Figure 5. Velocity vectors and
contaminant distribution in
TYPE 1 room model (1 supply &
4 exhausts, source: point A)

Figure 6. Comparison of diffusion
field for various source points
in TYPE 1 (simulation, source: point B~D)

(a) velocity vectors
    Experiment

(b) concentration : source A
    Experiment
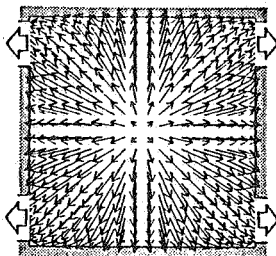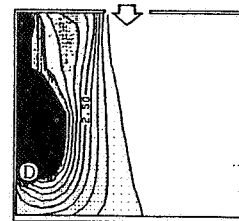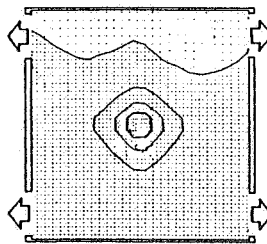
(c) velocity vectors
    Simulation

(d) concentration : source A
    Simulation
including supply openings (section)

(e) velocity vectors   (f) concentration : source A
    Simulation   Simulation
            near ceiling (plan)

(g) velocity vectors   (h) concentration : source A
    Simulation   Simulation
            near floor (plan)

Illustrated plane
      (Fig.7)   O :source

                        (a)~(d)   (e),(f)

       (plan)   (section)   (g),(h)

5.0   4.0   3.0   2.0   1.0   0'
Dimensionless concentration

Figure 7. Velocity vectors and contaminant distribution in TYPE 2 room model

(4 supplies & 4 exhausts, source: point A)

132

8.2 In the Case of Contaminant Generated between Supply Jet and Wall

Figure 6 shows the distributions of concentration in the case contaminant being generated between the supply jet and the wall at points B, C, and D, respectively. The generated contaminant is convected and diffused by the diverged flow near the floor and by the rising stream along the wall (Figure 6 (a), 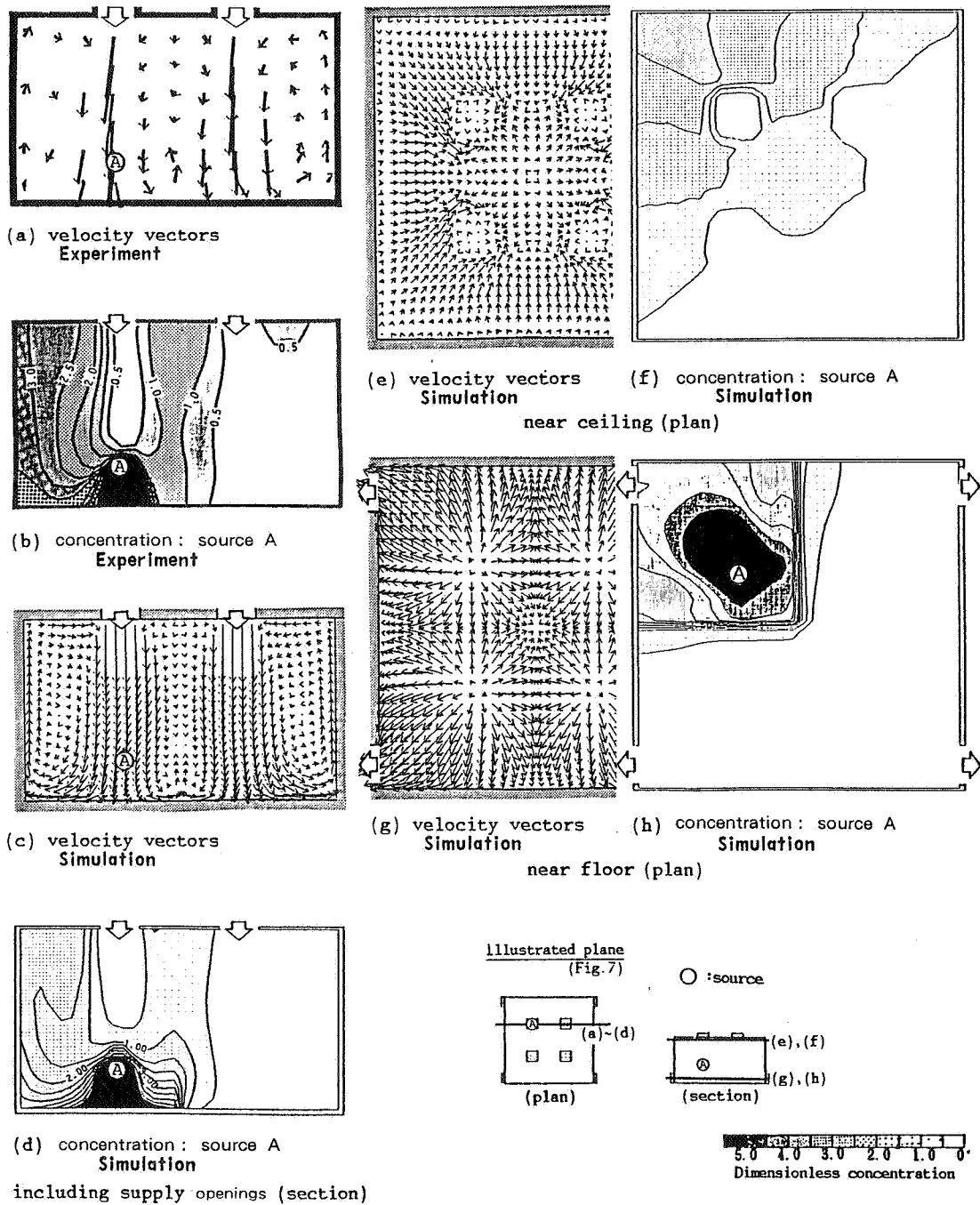(b), and (c)). When the air velocity is relatively weak at the source of the contaminant, it diffuses in all directions (Figure 6 (b)).The spatial average concentrations, SVE1, are 1.0 (in the case of point B), 1.3 (in the case of point C), 1.6 (in the case of point D). These values become larger as the source points are located closer to the wall. The mean radii of diffusion, SVE2, are 2.4 (in the case of point B), 2.3 (in the case of point C), and 2.1 (in the case of point D). These values become smaller as the sources are located nearer to the wall.
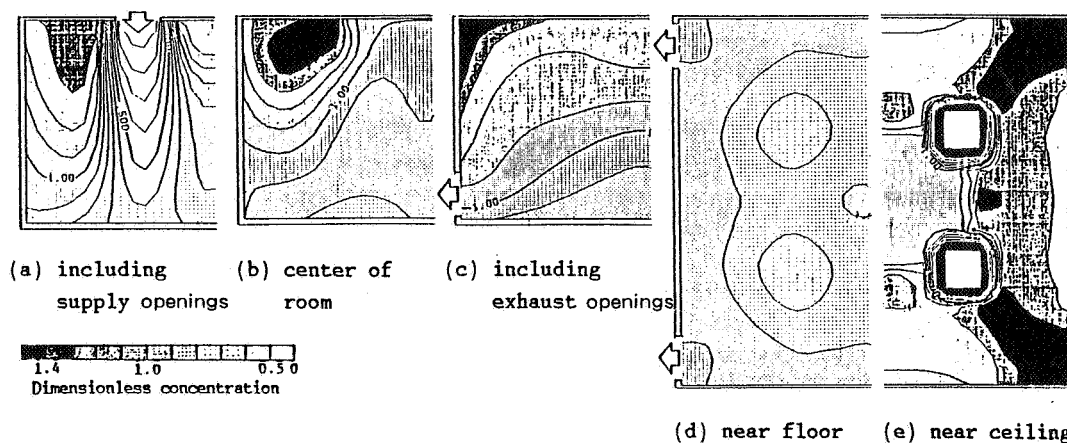
(a) including   (b) center of   (c) including
    supply openings   room   exhaust openings

1.4   1.0   0.5 0
Dimensionless concentration

(d) near floor   (e) near ceiling

Figure 8. Contaminant distribution (SVE3) in TYPE 2 (source: uniform generation throughout the room)

9. FLOW AND DIFFUSION FIELD FOR TYPE 2 (FOUR SUPPLY OPENINGS, Figures 7,8)

9.1 Characteristics of Flow Field

The distributions of velocity vectors in the several sectional planes are shown in Figure 7. Many characteristics of the flow pattern of Type 1 often appear in Type 2. It may be reasonable modeling to regard the flow pattern of Type 2 as a combination of four flow patterns of Type 1. The flow pattern of Type 1, which is characterized by a vertical down jet from the supply opening and the rising streams around it, might be called a 'flow unit,' each of which occupies a quarter space of Type 2.

9.2 In the Case of Contaminant Generated under Supply Opening

The supply jet hits the floor and diverges in all directions. Rising streams are formed between the area of supply openings and the area near the side walls (Figure 7(c)). The contaminant that is generated in the supply

133

jet spreads in accordance with this flow field. The concentration is the highest in the area from just below the source to the floor (Figure 5 (d)). The value of concentration is more than 0.5 only in the quarter part of the room that corresponds to the single 'flow unit' in which the contaminant is generated (Figure 7 (h)). In the remaining space of the room, concentration is very low (Figure 7 (d) and (h)). The spatial average concentration, SVE1, is 0.8 and is less than the value in the same case of Type 1. The mean radius of diffusion, SVE2, is 3, which is 25% of the relevant length of the room, 12.1, and is relatively less than the value in the same case for Type 1. These results are caused by the fact that the spreading area of the contaminant is confined to one 'flow unit'.

9.3 In the Case of Contaminant Generated Uniformly throughout Room, SVE3

Figure 8 shows the distribution of concentration in the case of the contaminant being generated uniformly throughout the room. The concentration takes its higher value around the supply openings, and at the corner of the ceiling, as shown in Figure 8. Thus, in terms of air mass movement, because the area around the supply opening is the farthest from the supply opening and the air mass takes the longest way to reach the area around the supply opening,the probability of the air around the supply opening being contaminated is the highest.
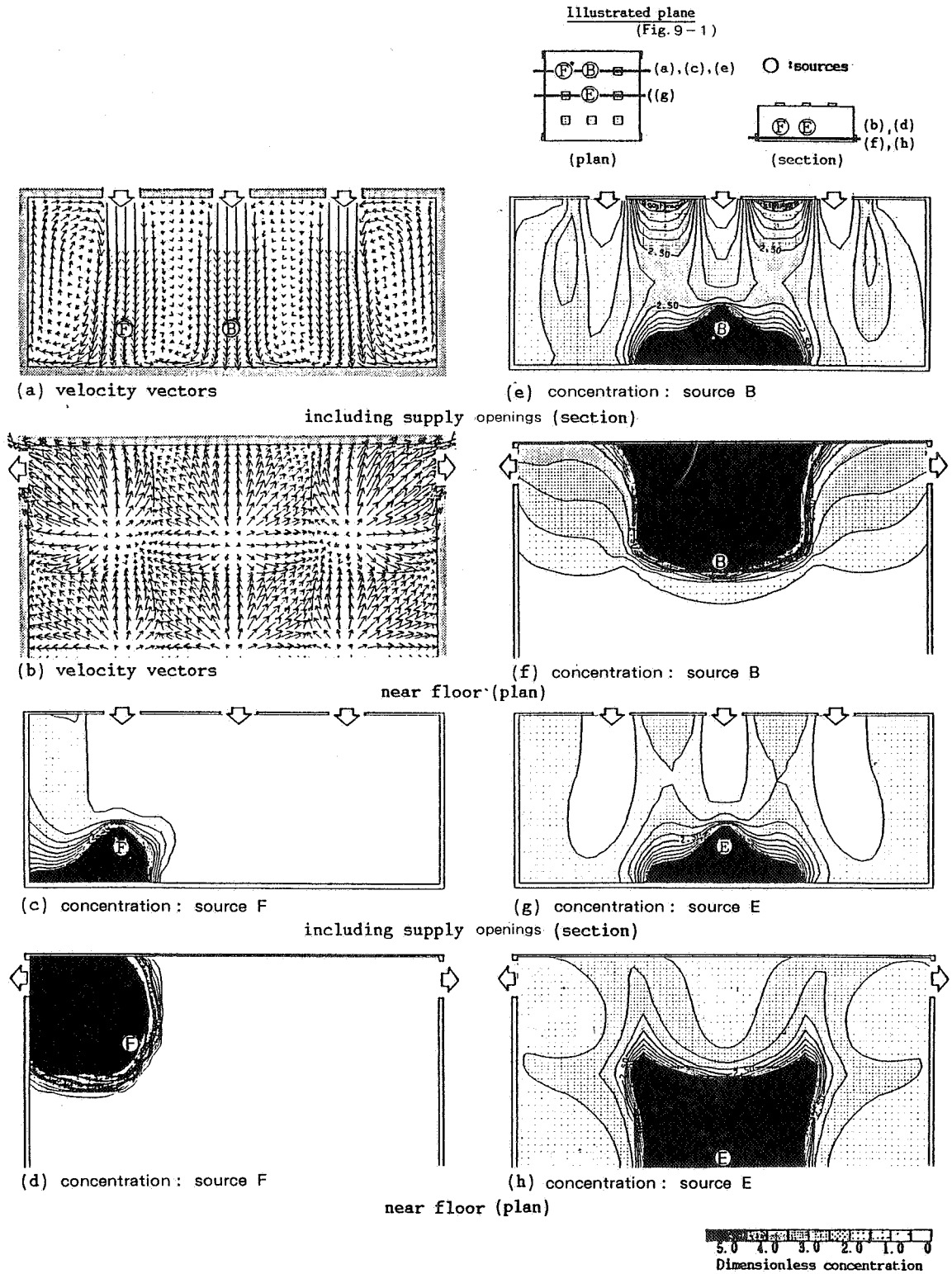
10. FLOW AND DIFFUSION FIELD FOR TYPE 4 (NINE SUPPLY OPENINGS, Figure 9,10)

10.1 In the Case of Contaminant Generated as Point Source

The flow field of Type 4 is shown in Figure 9-1(a),(b). As with Type 2 it is logical to regard the pattern of Type 4 as a serial combination of 'flow unit', in this case nine units. When the contaminant is generated in the flow unit that faces the exhaust opening (source point F, Figure 9-1(c) and (d)), the contaminant hardly diffuses into the other flow units, although the concentration is very high in that single flow unit. The spatial average concentration, SVE1, in this case is only 0.3 and the mean radius of diffusion, SVE2, is 2.3, 14% of the relevant room length of 16, showing very small value.

When the contaminant is generated in the center flow unit adjacent to the wall, (source point B, Figure 9-1(e) and (f)), the contaminant spreads, not only within that center flow unit, but also into the adjacent flow units that are located on the way to the exhaust opening. That one-third of the room is contaminated, but the remaining two-thirds of the room is very clean. The spatial average concentration, SVE1, is 1.2, and the mean radius of diffusion, SVE2, is 3.3. The latter value is considerably greater than that of the contaminant being generated at point F.

When the contaminant is generated in the center of the room at point E, all of the space is contaminated. Because this flow unit in which the contaminant is generated does not face the exhaust opening but is adjacent to all the other flow units, the contaminant is convected by the flow toward the exhaust through all the other flow units. The spatial average

Illustrated plane
(Fig. 9-1)

(a) velocity vectors
including supply openings (section)

(b) velocity vectors
near floor (plan)

(c) concentration : source F
including supply openings (section)

(d) concentration : source F
near floor (plan)

(e) concentration : source B

(f) concentration : source B

(g) concentration : source E

(h) concentration : source E

Dimensionless concentration
5.0 4.0 3.0 2.0 1.0 0

Figure 9-1. Velocity vectors and contaminant distribution in TYPE 4 room model
(9 supplies & 4 exhausts, source: point B,E,F)

135

(a) velocity vectors

(b) concentration : source A

(c) concentration : source B
center of room

(d) concentration : source D

(e) concentration : source E
center of room

Illustrated plane   Dimensionless concentration
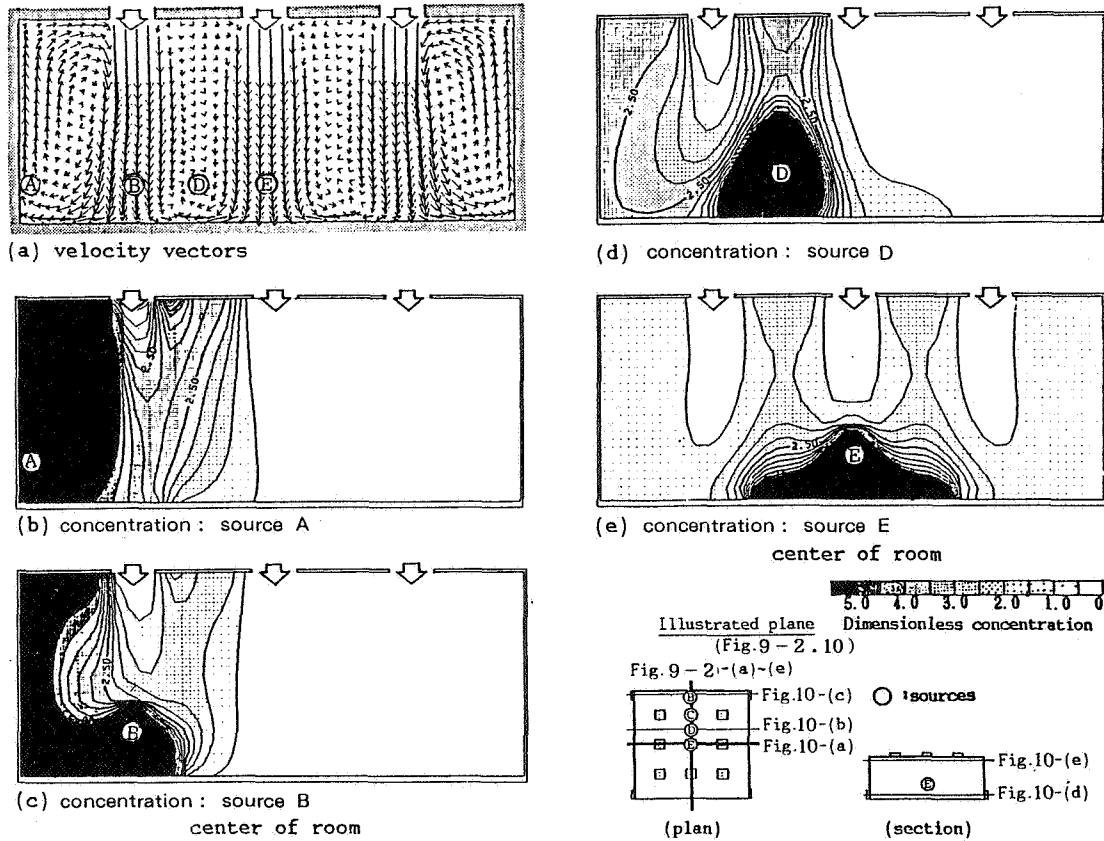(Fig.9 − 2 . 10)

Figure 9- 2. Comparison of contaminant distribution for various source points in TYPE 4
(source: point A~E)

concentration, SVE1, is 1.4, and the mean radius of diffusion, SVE2, is 4.3, 26% of the relevant length of the room.

Figure 9-2 shows the diffusion field when the contaminant is generated at point A, B, D, and E. These source points move from the area neighboring the wall to the center of the room. The spatial average concentrations, SVE1, are 1.7, 1.3, 1.4, and 1.4, respectively. The mean radii of diffusion, SVE2, are 3.1, 3.3, 3.6, and 4.3. Therefore, SVE2 becomes greater as the contaminant source is placed farther from the wall.

10.2   In the Case of Contaminant Generated Uniformly throughout Room, SVE3

Figure 10 shows the distribution of concentration of SVE3. The major characteristics of the concentration distribution pattern are almost the same as in the cases of Type 2. The highest value is observed near the ceiling around the supply opening and at the corners of the ceiling.
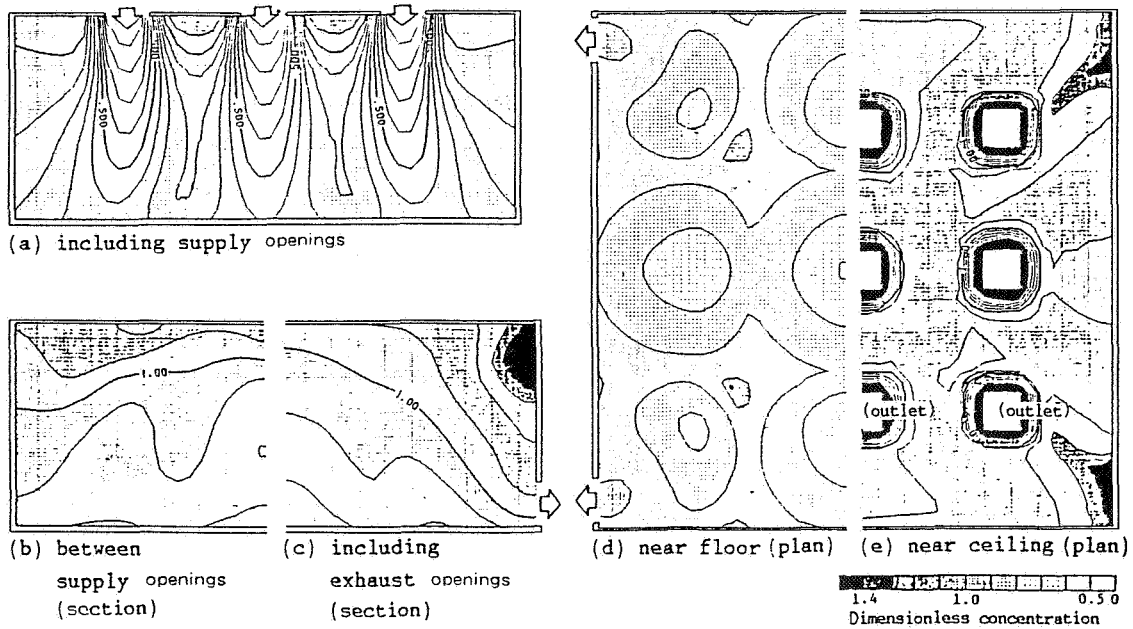
(a) including supply openings

(b) between supply openings (section)

(c) including exhaust openings (section)

(d) near floor (plan)

(e) near ceiling (plan)

1.4   1.0   0.5 0
Dimensionless concentration

Figure 10. *Contaminant distribution (SVE3) in TYPE 4 (source: uniform generation throughout the room)*

11.   CONCEPT OF 'FLOW UNIT'

From the results of the simulations, it may be concluded that the mean flow structure in the room that has supply openings in the ceiling is composed of series of flow units that consist of one supply jet and the rising streams around it. Such a flow unit is useful in comprehending the complicated flow pattern in rooms in which the supply openings are set in the ceiling. Furthermore, this concept of a flow unit seems to be helpful in comprehending the contaminant diffusion in rooms. It is a well-known fact that the exhaust flow has small influence on the whole flow pattern. Therefore, it is not defective that this model of a flow unit does not include the function of the exhaust opening.

When the contaminant is generated in a flow unit, the contaminant diffusion at its first stage is confined within that unit. If the flow unit faces the exhaust opening, the contaminant is not convected to the other flow units and only a small amount of the contaminant spreads to them by turbulent diffusion. If the contaminant is generated in the flow unit that does not face any exhaust openings, the contaminant is convected to the flow units that face the exhaust opening and the remaining flow units are not contaminated. Even if they do become contaminated, it is only to a small degree, because such contamination is caused solely by turbulent diffusion, which has much less ability to transport the contaminant than does mean flow convection. The turbulent Reynolds number (Peclet number), $U_0 L_0 / \nu$, in these cases is on the order of 100, which means in general that the ability to transport the contaminant by convection is a hundred times greater than that of turbulence diffusion.

137

When the contaminant is generated at the boundary of two flow units, where strong rising streams are usually formed, the contaminant diffuses into both and passes through the other flow units that are located on the path of the flow to the exhaust opening.

The qualitative characteristics of the structure of the diffusion field described above are quantitatively assessed very well by means of the new scales of ventilation efficiency SVE1,2 and 3.
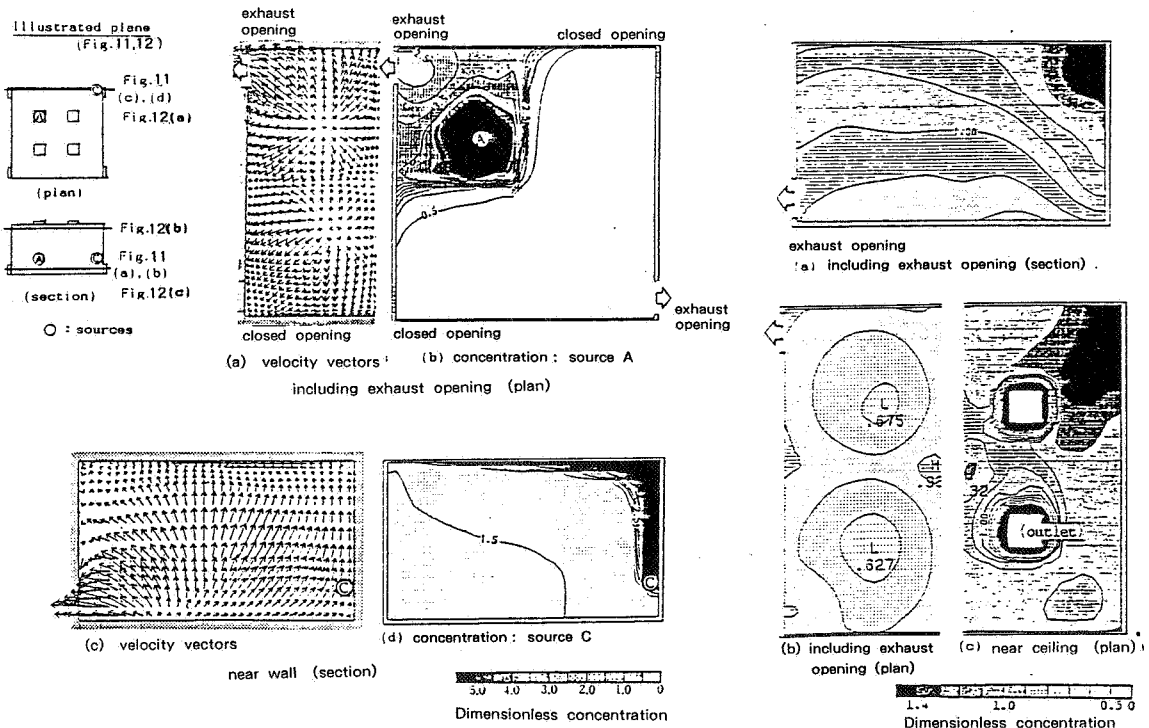

Figure 11. Velocity vectors and contaminant distribution in TYPE 3 (4 supplies & 2 exhausts)

Figure 12. Contaminant distribution (SVE3) in TYPE 3 (4 supplies & 2 exhausts, source: uniform generation throughout the room)

12. INFLUENCE OF ARRANGEMENT OF EXHAUST OPENINGS (TYPE 2,3, Figures 7,11,12)

Type 3, in which two exhaust openings are located diagonally, is a room model derived from Type 2 and is regarded as a case of decreasing exhaust openings. In this room model, only two exhaust openings are located at diagonal corners (the other two exhaust openings are eliminated). As shown in Figure 11(a), there are four 'flow units' in this type as well as in Type 2 (Figure 7). In the case of contaminant generation at point A, which is in the 'flow units' adjacent to the exhaust opening and is under the supply opening, although the contaminated space is nearly the same as with Type 2 (cf.Figure 7(h) and 11(b)) and the value of the mean radius of diffusion, SVE2, is the same, the value of the spatial average concentration, SVE1, for Type 3 is smaller than that for Type 2, which means that the contaminant is exhausted effectively by the stronger flow toward the exhaust opening.

138

At the corner of the eliminated exhaust openings, strong rising streams along the wall appear. When the contaminant is generated in this position (point C), the contaminant spreads upward along the wall and the large area along the ceiling becomes highly contaminated (cf. Figure 11(c) and 11(d)). In this case, the values of the spatial average concentration, SVE1, and the mean radius of diffusion, SVE2, are higher than for all other cases in this room model (1.6 and 3.4 respectively). The distribution of the concentration in the case of uniform contaminant generation throughout the room is shown in Figure 12. At the corner near the ceiling of the upper position of the closed exhaust openings, the concentration becomes very high.

13. INFLUENCE OF SYSTEMATIC CHANGE OF ARRANGEMENT OF SUPPLY OPENING (TYPE 4,5,6,7,8, Figures 13,14)

In this section, flow and contaminant diffusion fields in the same room with different arrangements of supply openings (Type 4,5,6,7,8) are compared. These supply arrangements, in which the numbers are progressively decreased, are modeled on the basis that the air exchange rate is decreased according to the elimination of supply openings rather than by decreasing the supply air volume of each opening.

Figure 13 shows the flow field and contaminant diffusion field in the case where the contaminant is generated at the center of the room (Point E). The outline of the structure of the flow units is illustrated in each superimposed figure using broken circles.

13.1 Flow fields and Contaminant Diffusion Fields in Case of Contaminant Generated at point E

(1)   Type 4 (Figure 13(a)-(c)).

There are nine flow units in the room model, and rising streams appear at the boundary of each flow unit. The rising streams in the space between the two closest jets do not reach the ceiling. Since the contaminant is generated in a supply jet, the highly contaminated region spreads under source point E. The flow unit that includes the contaminant source is highly contaminated.

(2)   Type 5 (Figure 13(d)-(f)).

Six flow units comprise the total flow field. At the centerline of the room, where three supply openings are closed, strong rising streams appear toward the ceiling. This centerline corresponds to the boundary of the expanded flow units. Since the contaminant is generated in this rising stream, the highly contaminated region spreads upward from source point E. The whole room is filled with highly contaminated air.

(a) velocity vectors

(b) concentration (Model 1)
center of room (section)

TYPE 4 (9 supplies & 4 exhausts)

(c) concentration
including exhaust opening (plan)

(d) velocity vectors

(e) concentration (Model 1)
(section)

TYPE 5 (6 supplies & 4 exhausts)

(f) concentration (plan)

(g) velocity vectors

(h) concentration (Model 1)
(section)

TYPE 6 (5 supplies & 4 exhausts)

(i) concentration (plan)

(j) velocity vectors

(k) concentration (Model 1)
(section)

TYPE 7 (4 supplies & 4 exhausts)

(1) concentration (plan)

(m) velocity vectors

(n) concentration (Model 1)
(section)

TYPE 8 (1 supply & 4 exhausts)

(o) concentration (plan)

5.0 4.0 3.0 2.0 1.0 0
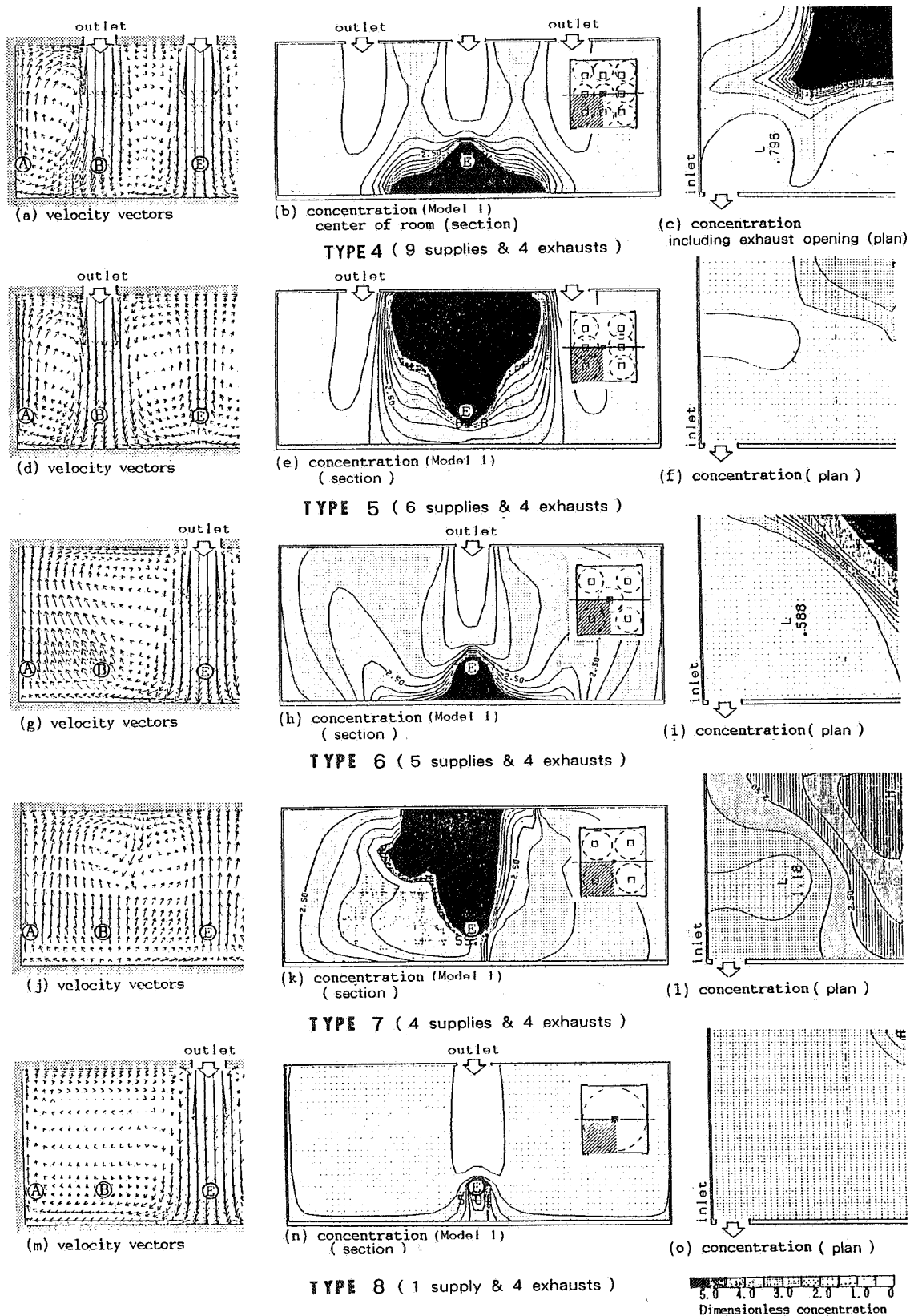Dimensionless concentration

**Figure 13. Effect of decreasing supply openings on diffusion field
(TYPE 4-8, source: point E)**

140

(3)   Type 6 (Figure 13(g)-(i)).

The five checkered flow units comprise the total flow field. The rising streams surrounding the center flow unit spread toward the upper position of the walls. Since the contaminants are generated in the supply jet in the center flow unit, the highly contaminated region appears under source point E. This contaminated air is transported by the rising flow toward the upper position of the walls and most of the space becomes contaminated. The concentration becomes more than 1.0 in most of the space.

(4)   Type 7 (Figure 13(j)-(l)).

Four large flow units comprise the total flow field. At the center of the room, a narrow rising stream appears toward the ceiling. Since the contaminant is generated in the rising stream, the highly contaminated region spreads above source point E, and most of the room is filled with contaminated air. In this simulation, the contaminant diffusion field is slightly asymmetric because of the asymmetry of the flow field due to numerical instability.

(5)   Type 8 (Figure 13(m)-(o)).

There is only one flow unit in the room model. Since the contaminant is generated in the supply jet, the highly contaminated region spreads under source point E. The concentration is more than 1.5 throughout the whole room except for the area around the clean supply jet.

13.2   Comparison of Location of Supply Openings Concerning Ventilation Effectiveness
(Source Point E)

In Table 4 two kinds of averaged spatial concentration (Model 1 and 2) and the mean radius of diffusion are tabulated for each type. Model 1 is a dimensionless concentration which is normalized by the mean concentration, Co, for each type. Model 2 is also a dimensionless concentration which is normalized by the mean concentration of Type 4 commonly.

The supply air velocity is the same for all types. Therefore, the air exchange rate is naturally different for each type. In Model 1, the representative concentration (C_o) for non-dimensionalization is not the same. But in Model 2, the representative concentration (C_o) of Type 4 is used in common for making the dimensionless value.

Figure 14(a) shows the spatial average concentration of each type for source point E. In this figure, the dimensionless concentration of Model 2 is shown. The hyperbolic curve expresses the dimensionless average spatial concentration of Type 4 in which the air exchange rate is gradually decreased under the condition of a constant generation rate. We can thus comprehend the ventilation effectiveness of the different arrangements of the supply openings. Using this figure, if the plotted point of average spatial concentration for a type is below the hyperbolic curve, the ventilation effectiveness of that type is superior to that of Type 4 under

(a) Spatial averaged concentration with respect to air exchange rate for source point E

(b) for source point B

(c) for source point A
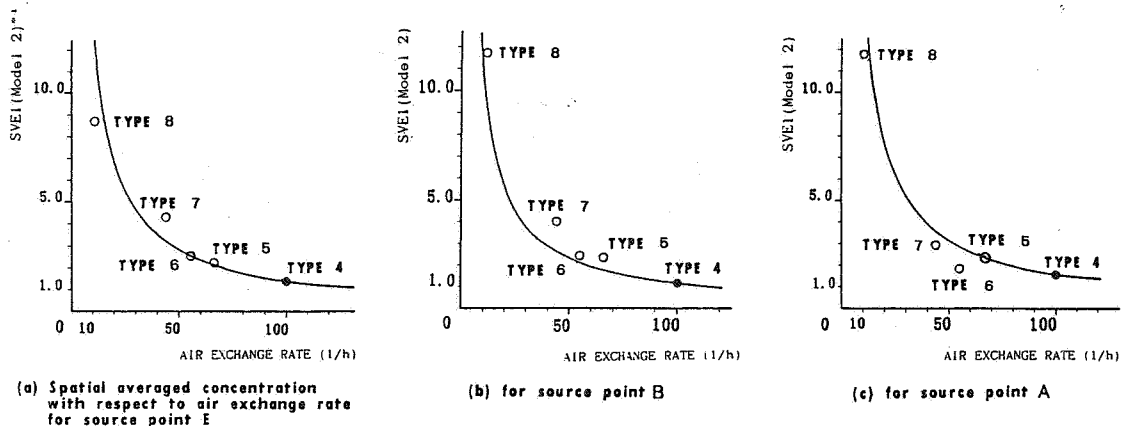
*1 SVE1 : spatial averaged concentration.
*2 Contaminant generation rate for each type is same as in TYPE 4.

Figure 14. Comparison of ventilation efficiency based on SVE1 by decreasing supply openings

Table4. Values of spatial averaged concentration (SVE 1) and Mean radius of Diffusion (SVE 2) for TYPE 4~8

sources	point E (center of room)			point B (between center and wall)			point A (near the wall)		
Scales of Ventilation Efficeincy	SVE 1 (Model 1)	SVE 1 (Model 2)*¹	SVE 2 (*²)	SVE 1 (Model 1)	SVE 1 (Model 2)	SVE 2	SVE 1 (Model 1)	SVE 1 (Model 2)	SVE 2
TYPE 4	1.4	1.4	4.2	1.3	1.3	3.3	1.7	1.7	3.1
TYPE 5	1.5	2.3	4.0	1.6	2.3	4.1	1.7	2.5	4.0
TYPE 6	1.4	2.5	4.3	1.4	2.5	3.8	1.0	1.9	4.0
TYPE 7	1.9	4.3	3.8	1.8	4.1	3.8	1.3	2.9	4.0
TYPE 8	1.0	8.7	3.9	1.3	11.8	4.3	1.3	11.6	4.3

* 1 : Model 2 is dimensionless concentration in which the mean concentration of TYPE4 is commonly used as the representations value for non − dimensionalization.

* 2 : Dimensionless length : these values are made dimensionless by dividing by the width of the supply opening (0.6m).

the same air exchange rate. This corresponds to the comparison based on Model 1, since the comparison based on Model 1 assumes the same air exchange rate and the same contaminant generation rate.

As shown in Figure 14(a), for the contaminant source point E, ventilation effectiveness among these different supply opening arrangements may be judged in the following order: Type 8 > Type 4 = Type 6 = Type 5》 Type 7 (cf. comparison of SVE1 based on Model 1 in Table 4).

For the mean radius of diffusion Type 4 and Type 6 have rather high values (cf. Table 4). The contaminant source point in all these cases is located in the supply jet.

13.3   Comparison of Location of Supply Openings Concerning Ventilation Effectiveness
        (Source Point B)

For the case of source point B (cf. Figure 13), two kinds of average spatial concentration (Models 1 and 2) and the mean radius of diffusion are tabulated for each type in Table 4 and comparisons of ventilation effectiveness are shown in Figure 14 (b) in the same manner as before.

Since every plotted point of the average spatial concentration in Type 5 - Type 8 room model is above the hyperbolic curve, it may be concluded that the arrangement of the supply openings in Type 5 - Type 8 for this contaminant source is inferior to that of Type 4 under the same air exchange rate. For contaminant source point B, ventilation effectiveness among these different cases of arrangement of supply openings is estimated in the following order: Type 4 = Type 8 > Type 6 > Type 5 > Type 7.

For the values of the mean radius of diffusion, there seems to be small difference among them.

13.4   Comparison of Location of Supply Openings Concerning Ventilation Effectiveness
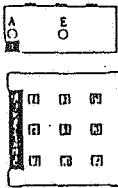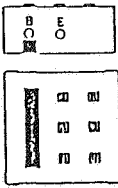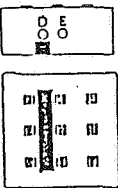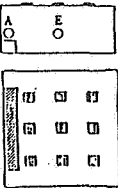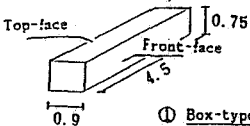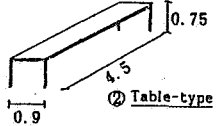   (Source Point A)

For the case of source point A (cf. Figure 13), two kinds of average spatial concentration and the mean radius of diffusion are tabulated for each type in Table 4; comparisons of ventilation effectiveness are shown in Figure 14 (c) as before.

Since the plotted points of the averaged spatial concentration of Type 6 and Type 7 are below the hyperbolic curve, it may be concluded that for this contaminant source, the arrangements of the supply openings in Type 6 and Type 7 are superior to that of Type 4 under the same air exchange rate from the viewpoint of ventilation effectiveness. Note especially that Type 6, which has only five-ninths the air exchange rate of Type 4, has almost equal ventilation effectiveness with Type 4. Thus, for contaminant source point A, ventilation effectiveness among these different arrangements of supply openings is estimated in the following order: Type 6 ≫ Type 7 = Type 8 > Type 4 = Type 5.

The values of the mean radius of diffusion for these room models, except for Type 4, are close to 4.0 and thus larger than Type 4 (3.1: cf. Table 4)

The room model used here is Type 4 which has 9 supply openings and 4 exhaust openings. Table 5 lists the four cases analyzed here and illustrates the various arrangements of flow obstacles and various source positions of contaminant.
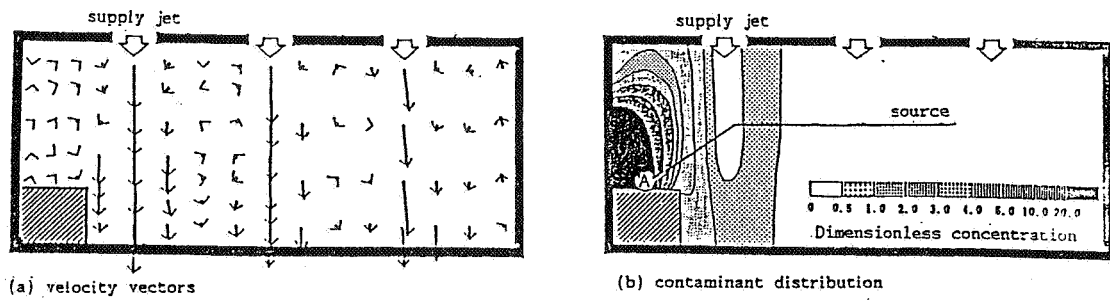
Table 5. Specifications of Cases of Air Flow with Obstacles

Cases	Case 1	Case 2	Case 3	Case 4
Flow Obstacles	One Box-type Obstacle	One Box-type Obstacle	One Box-type Obstacle	One Table-type Obstacle
Arrangement of Flow Obstacles and Position of Contaminant Generation (shown by the circle in the section)	(In contact with the wall)	(under suply jets)	(between supply jets)	(in contact with the wall)
Position of Contaminant Generation	A:adjacent to the wall (on the top-face of obstacle) E:center of the room S:SVE3	B:under supply jet E:center of the room S:SVE3	D:between supply jets E:center of the room S:SVE3	A:adjacent to the wall E:center of the room S:SVE3

① Box-type

② Table-type

remarks   1 Numerical simulations were conducted for all cases.
          2 Model experiment was conducted only for case 1.

14.1   Arranging a Box-Type Obstacle in Contact with the Side Wall (Case 1, Figures 9,10,15,16,17)

The velocity field and the contaminant diffusion field with a flow obstacle in contact with the side wall as given by numerical simulation are shown in Figures 16 and 17. The results of the experiment for this case are shown in Figure 15. As stated before, the correspondence between the simulation and the experiment is rather well. The standard case with no flow obstacle is shown in Figure 9. The designated names for each face of the obstacle used here are also illustrated in Table 5.

supply jet

(a) velocity vectors

supply jet

source

0 0.5 1.0 2.0 3.0 4.0 5.0 10.0 20.0

Dimensionless concentration

(b) contaminant distribution

(a),(b) : sections at center of the room

**Figure 15. Velocity vectors and contaminant distribution in Case 1 (TYPE4)
given by model experiment**

(Case 1: A box-type obstacle is placed in contact with the wall)

supply jet

(a) section : center of the room

(c) plan : near the top-face of obstacle

(b)

exhaust

(a)

(c)
(d)

Illustrated plane

(b) section : in front of the wall

Top-face

Back-face   Front-face

(d) plan : near the floor
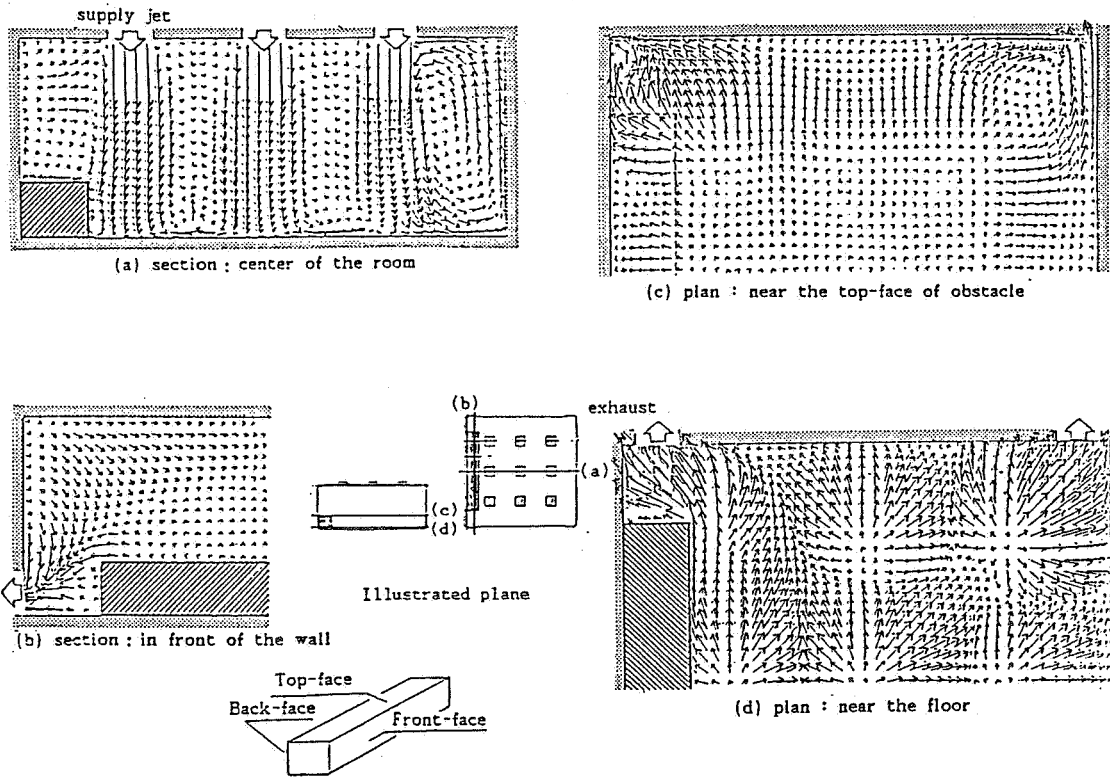
Figure 16. Velocity vectors in Case 1 (TYPE4) given by numerical simulation

145

(a) source : point A
(center section of the room)

(c) source : point E
(center section of the room)

(e) source : throughout the room
(center section of the room)

0.5 0.6 0.7 0.8 0.9 1.0 1.1 1.2 1.3
Dimensionless concentration : (e)

(b) source : point A
(plan near the floor)

(d) source : point E
(plan near the floor)

0.5 1.0 1.5 2.0 2.5 3.0 3.5 4.0 4.5
Dimensionless ·concentration : (a)~(d)

(b)(d)

(a)(c)(e)

Illustrated plane

Figure 17. Contaminant distributions in Case 1 given by numerical simulation

(1) Velocity Field.

The flow pattern in front of the side wall is illustrated in Figure 16(b). As shown in Figure 16(a), a recirculating flow appears above the obsta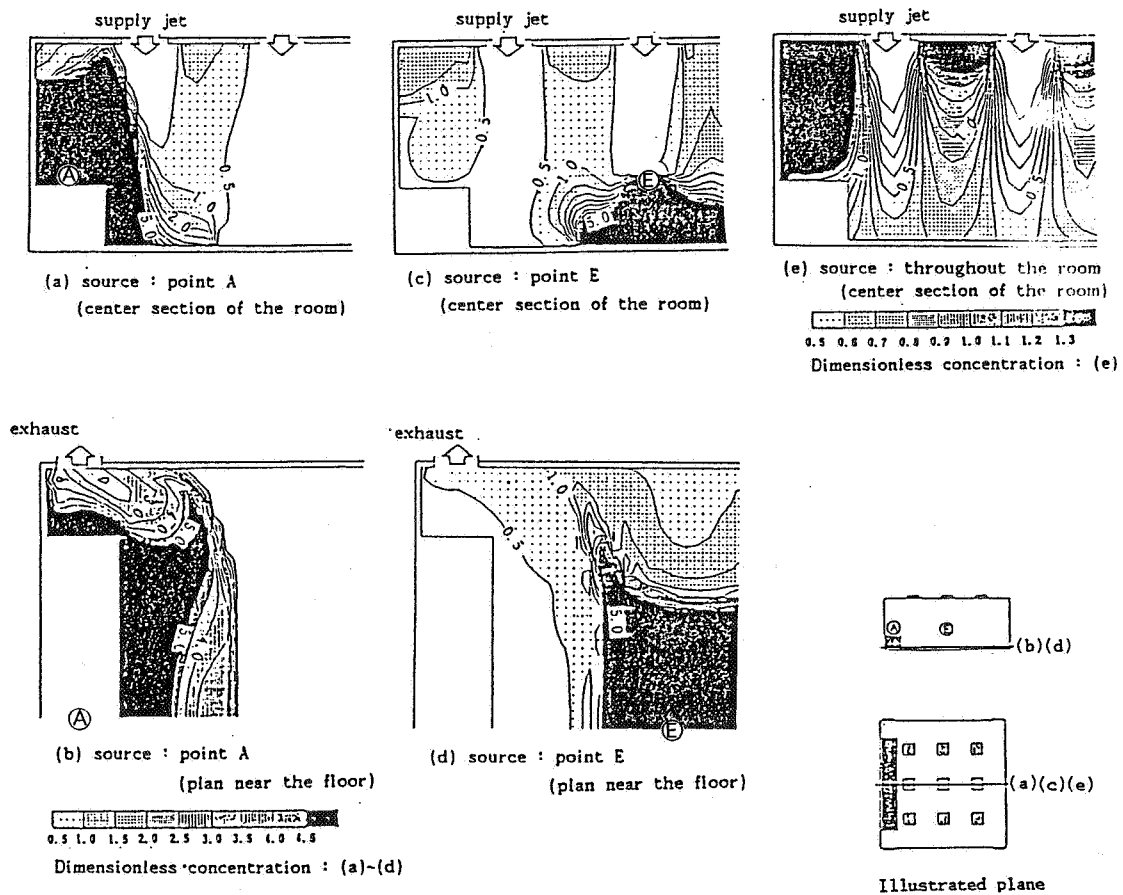cle and some flows into the supply jet near the ceiling. The air above the top-face of the obstacle moves towards the side wall as shown in Figures 16(a),(c). In front of the obstacle, the air moves towards the exhaust opening along the front-face of the obstacle as shown in Figure 16(d).

The airflow pattern near the side wall with no obstacle is also shown in Figure 9-1. It differs greatly from that of Case 1. In the open area on the right side far from the obstacle, there is little difference between the two. The conspicuous effect of the flow obstacle is confined within the space around the obstacle, namely within the 'flow units' in which the obstacle exists.

(2) Contaminant Concentration Field.

When the contaminant is generated on the top-face of the obstacle (Point A, Figures 17(a),(b)), the contaminant diffuses into the left third of the

146

room. This one-third diffusion pattern is similar to the result without obstacle. The concentration near the ceiling becomes rather low since the clean air is convected along the ceiling from the corner area. The value of SVE1 is 2.1 which is much larger than its value in the case without obstacle (1.7). The value of SVE2 is 2.5, smaller than in the case without obstacle (3.1). The values of SVE1 and 2 for all cases are tabulated in Table 6.

When the contaminant is generated in the center of the room (Point E, Figures 17 (c),(d)), it spreads throughout the whole room. But the space around the obstacle is not contaminated because air from the three supply jets near the side wall flows into this area. The value of SVE1 is 1.6 and hence larger than in the case without obstacle (1.4). Thus the ventilation efficiency for exhausting the contaminant decreased to some degree in Case 1. The value of SVE2 in Case 1 is 4.3, almost the same as the case without obstacle (4.2). Although the obstacle beside the wall has small effect on the velocity field around point E, the diffusion field for contaminant generation at Point E is influenced greatly whether the flow obstacle is present or not.

The value of SVE3 is compared in Figure 17(e) and Figure 10(a). The concentration above the obstacle in Case 1 is much higher than in the case without obstacle, thereby indicating that supplied clean air requires a long travelling time to reach this recirculating area around the obstacle.

14.2   Arranging a Box-type Obstacle Under Supply Jets (Case 2, Figures 18,19)

The velocity and diffusion fields when a flow obstacle is placed under the supply jets are shown in Figures 18 and 19.

(1)   Velocity Field.

The supply jet attacks the top-face of the obstacle and diverges in all directions (Figures 18(a),(c)). A small rising stream appears above the top-face between the supply jets (Figure 18(b)). Recirculating flows exist in front of the back and front-faces of the obstacle(Figure 18(a)). In the open area on the right, the velocity field of Case 2 is the same as that of the case without obstacle, hence the significant effect of this arrangement of the flow obstacle is confined within a rather small area near the obstacle.

(2)   Contaminant Diffusion Field.

When the contaminant is generated at the top-face of the obstacle (Point B), it is convected horizontally by the diverging flow at this area (Figure 19(a)). The high concentration spreads into the recirculating region along the side wall and also into the area in front of the back and front-faces (Figure 19a)). The contaminated area occupies the left half of the room (Figures 19(a),(b)). The value of SVE1 in Case 2 is 1.9 and much larger than in the case without obstacle (1.3). The value of SVE2 in Case 2 is 3.7 and also larger than in the case without obstacle (3.2).

When the contaminant is generated at the center of the room (Point E), it spreads into the open area on the right where no obstacle is arranged (Figures 10(c),(d)). The space to the left of the obstacle is clean since
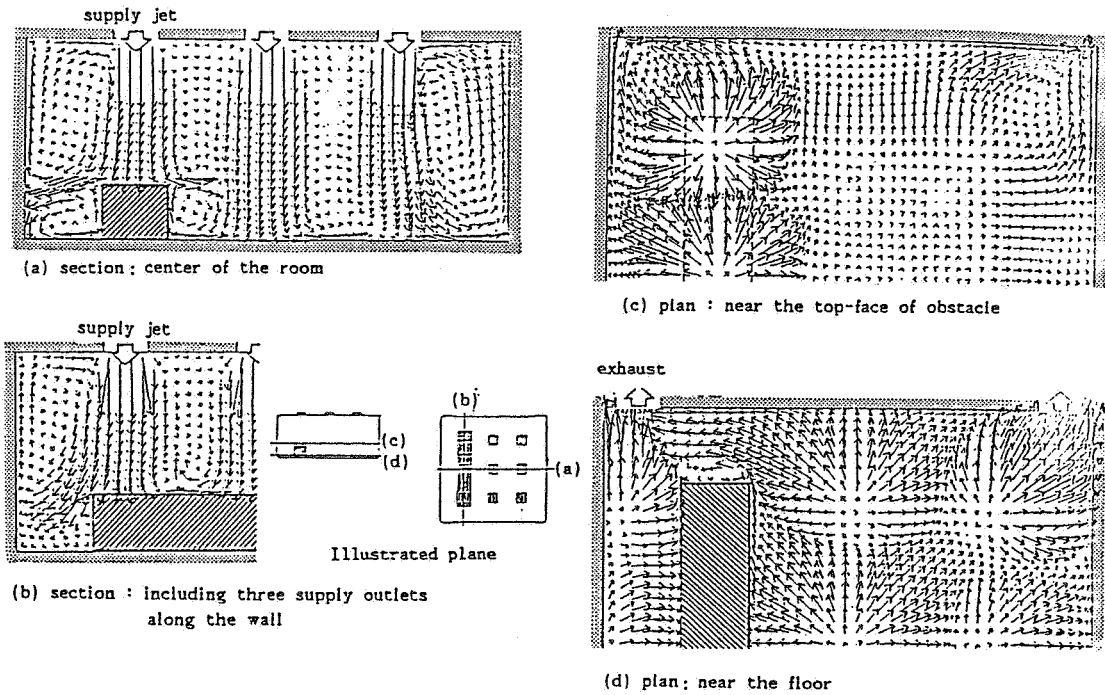
supply jet

(a) section: center of the room

supply jet

(b) section: including three supply outlets
along the wall

Illustrated plane

(b)
(c)
(d)
(a)

(c) plan : near the top-face of obstacle

exhaust

(d) plan: near the floor

Figure 18. Velocity vectors in Case 2

(Case 2: A box-type obstacle is placed under supply jets)

supply jet

(a) source : point B
(center section of the room)

exhaust

(b) source : point B
(plan near the floor)

supply jet

(c) source : point E
(center section of the room)

exhaust

(d) source : point E
(plan near the floor)

Dimensionless ·concentration : (a)~(d)
0.5 1.0 1.5 2.0 2.5 3.0 3.5 4.0 4.5

supply jet

(e) source : throughout the room
(center section of the room)

0.5 0.6 0.7 0.8 0.9 1.0 1.1 1.2 1.3
Dimensionless concentration : (e)

(b)(d)

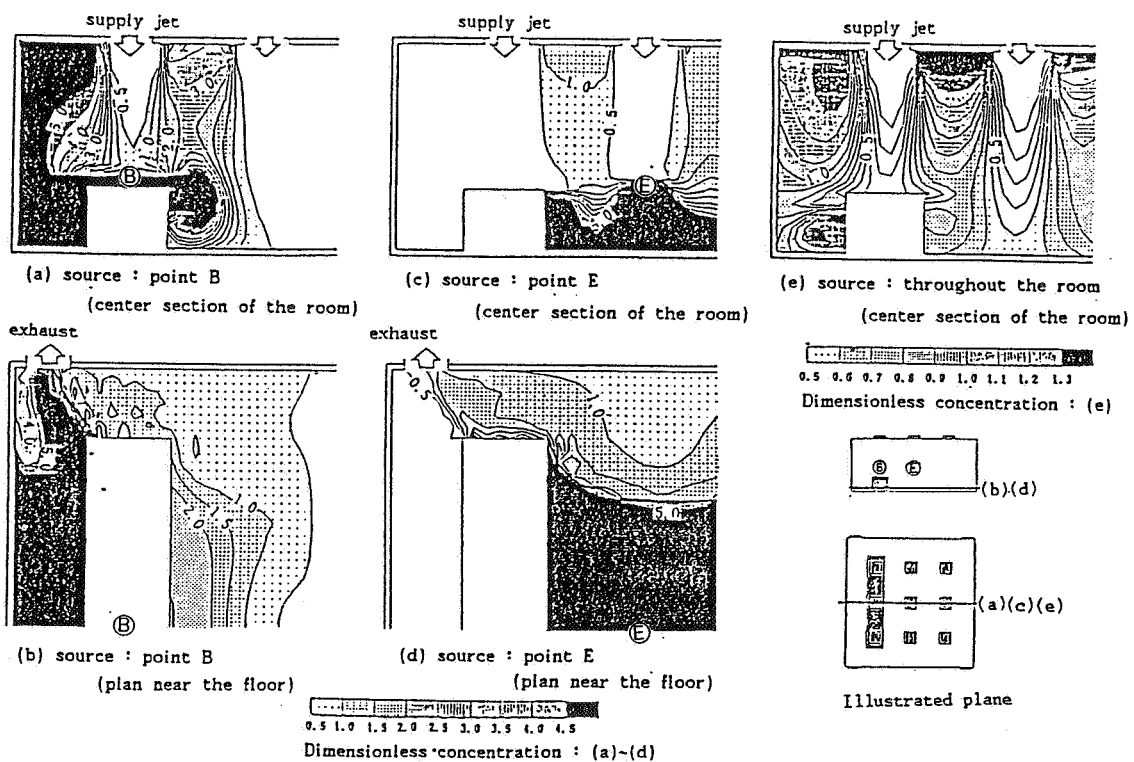Illustrated plane

(a)(c)(e)

Figure 19. Contaminant distributions in Case 2 with various source position

148

the spread of the contaminant is blocked by the obstacle. The value of SVE1 is 1.6 and larger than in the case without obstacle (1.4). The value of SVE2 is 4.2, which is the same as in the case without obstacle (4.2).

The value of SVE3 is very low above the top-face of the obstacle because of the direct supply of clean air (Figure 19(e)).

14.3 Arranging a Box-Type Obstacle Between Supply Jets (Case 3, figures 20,21)

The flow and diffusion fields for Case 3 are illustrated in Figures 20 and 21, where a box-type obstacle is arranged between the supply jets.

(1) Velocity Field.

The velocity field at the top-face of the obstacle is horizontal and flows mainly towards the exhaust opening, as shown in Figures 20(a),(c). Rising streams appear at some points above the obstacle (Figure 20(b)). The supply jets at the center attack the floor and thus diverge towards the open area on the right because of blocking on the left side by the obstacle. The flow pattern in the open area on the right side is similar to that in the case without obstacle.

(2) Contaminant Diffusion Field.

When the contaminant is generated on the top-face of the obstacle (Point D, Figure 21(a)), it stays around the obstacle since the diffusion field is blocked by the rows of the supply jets on both sides of the obstacle (Figure 21(a)). The contaminated area is the left half of the room(Figures 21(a),(b)). The value of SVE1 is 1.7, which is larger than in the case without obstacle (1.5). The value of SVE2, on the other hand, is 3.2 and significantly smaller than in the case without obstacle (3.6).

When the contaminant is generated at the center of the room (Point E), it diffuses into the right half of the room, since diffusion towards the left is blocked by the obstacle (Figures 21(c),(d)). The top-face of the obstacle is clean since the supply jet attacks it. The value of SVE1 is 1.5 and a little larger than in the case without obstacle (1.4). The value of SVE2 (4.0) on the other hand is smaller than in the case without obstacle (4.2).

The distribution of SVE3 (Figure 21(e)) is similar to that in the Case without obstacle.

14.4 Arranging a Table-Type Obstacle (Case 4, Figures 22,23)

The flow and diffusion fields for Case 4 where a table-type obstacle is placed in contact with the side wall are illustrated in Figures 22 and 23.

(1) Velocity field.

A large recirculating flow appears above the obstacle (Figure 22(a)). The airflow pattern on the top-face is shown in Figure 22(c). The air under the top-face moves along the side wall and towards the exhaust opening (Figures 22(b),(d)). The flow pattern in the open area on the right side is the same as in the case without obstacle (Figure 22(a)). Thus the area affected by
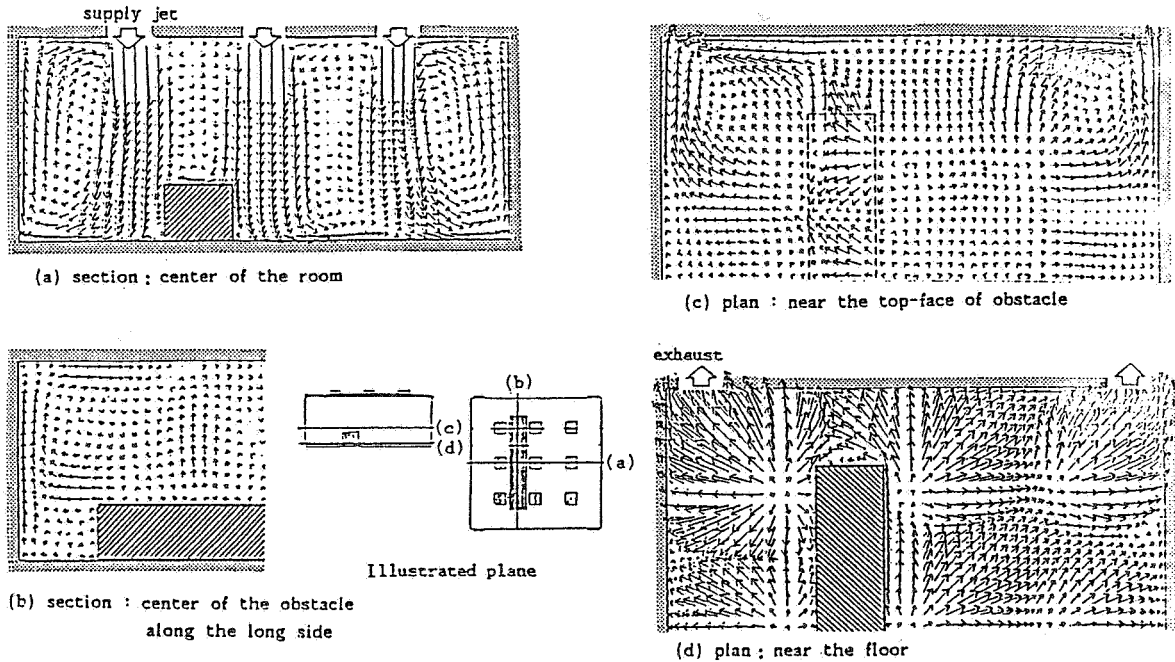
(a) section : center of the room

(c) plan : near the top-face of obstacle

(b) section : center of the obstacle
along the long side

Illustrated plane

(d) plan : near the floor

Figure 20.   Velocity vectors in Case 3

(Case 3: A box-type obstacle is placed between supply jets)

(a) source : point D
(center section of the room)

(c) source : point E
(center section of the room)

(e) source : throughout the room
(center section of the room)

Dimensionless concentration : (e)

(b) source : point D
(plan near the floor)

(d) source : point E
(plan near the floor)

Dimensionless concentration : (a)~(d)

Illustrated plane
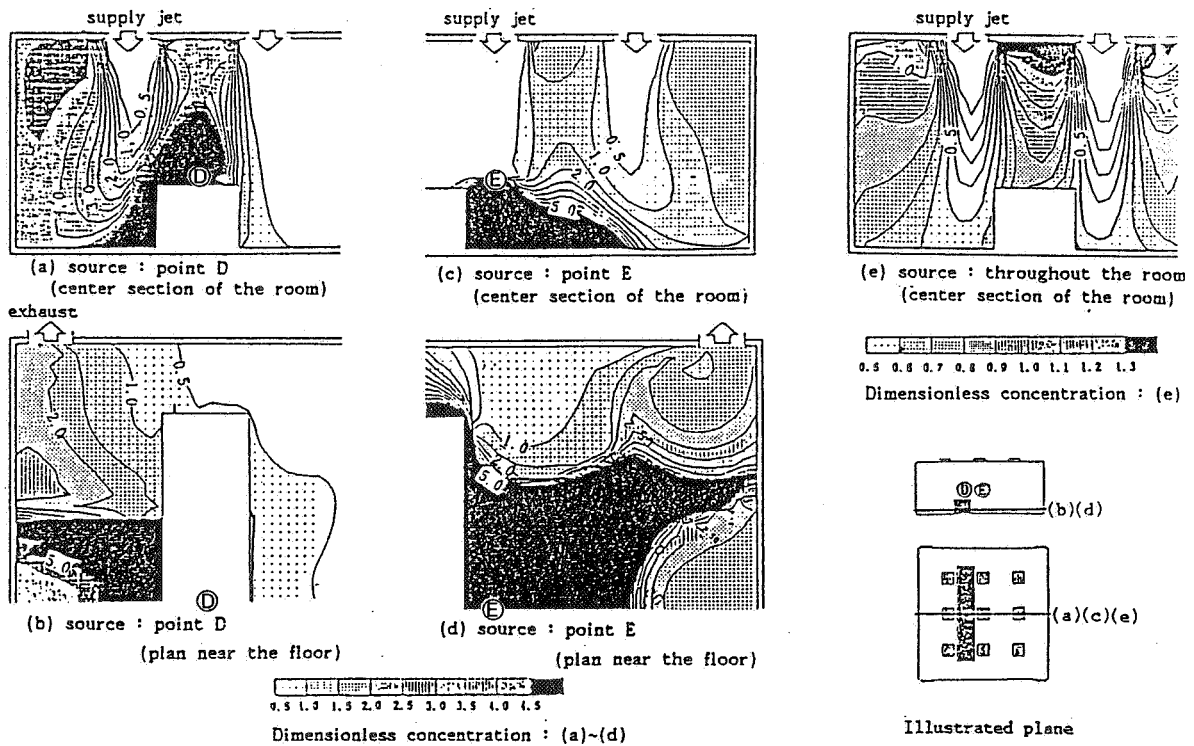
Figure 21.   Contaminant distribution in Case 3 with various source position

150

(a) section : center of the room

(b) section : in front of the wall

Illustrated plane

(c) plan : near the top-face of obstacle

(d) plan : near the floor
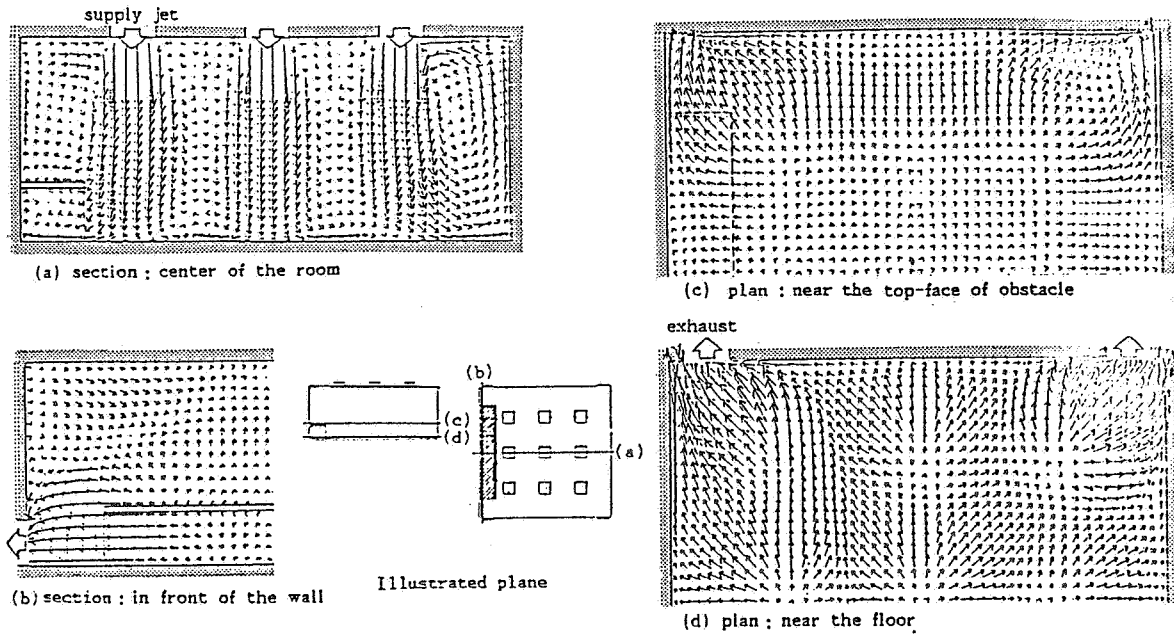
Figure 22. Velocity vectors in Case 4

(Case 4: A table-type obstacle is placed in contact with the wall)

(a) source : point A
(center section of the room)

(b) source : point A
(plan near the floor)

(c) source : point E
(center section of the room)

(d) source : point E
(plan near the floor)

Dimensionless concentration : (a)~(d)

0.5 1.0 1.5 2.0 2.5 3.0 3.5 4.0 4.5

(e) source : throughout the room
(center section of the room)

Dimensionless concentration : (e)

0.5 0.6 0.7 0.8 0.9 1.0 1.1 1.2 1.3

(b)(d)
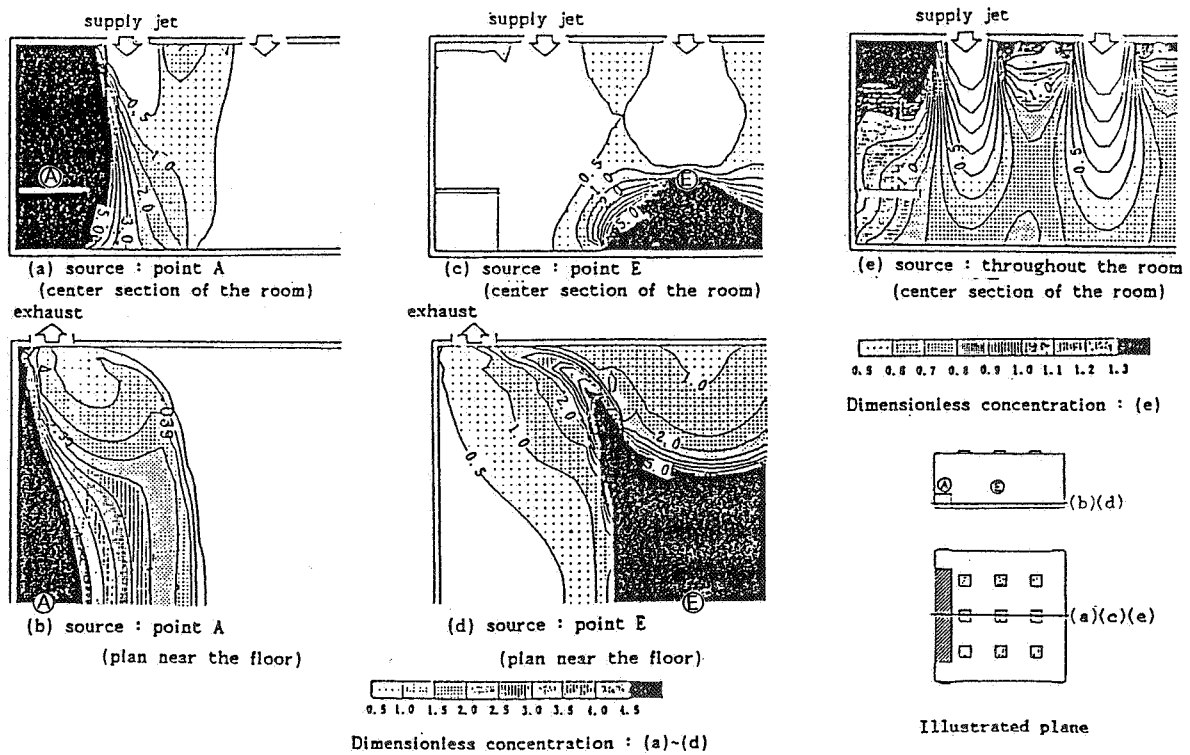
(a)(c)(e)

Illustrated plane

Figure 23. Contaminant distributions in Case 4 with various source position

the obstacle is rather small and is confined within the area around the table.

(2) Contaminant Diffusion Field.

When the contaminant is generated on the top-face of the table (Point A), the region from the floor to the ceiling is contaminated highly (Figures 23(a),(b)). But the contaminated area is limited to the left third of the room. The value of SVE1 in this case is 1.4 and much smaller than in Case 1 (2.1). Hence the flow field with a table-type obstacle is much more efficient to exhaust contaminant than that with a box-type obstacle. The value of SVE2 in this case is 2.5 and the same as in Case 1 (2.5).

When the contaminant is generated at the center of the room(Point E), it spreads around the center near the floor (Figures 23(c),(d)). The air around the table is very clean since the three supply jets along the side wall attack the table. The value of SVE1 is 1.3 and considerably smaller than in Case 1 (1.6). It can thus be concluded that a table-type obstacle is superior to a box-type obstacle from the view point of ventilation efficiency of SVE1. The value of SVE2 is 4.2 and the same as in Case 1 (4.3).

The value of SVE3 (Figure 23(e)) is high in the area above the obstacle, particularly near the ceiling, but it is smaller than in Case 1 (Figure 17(e)).

14.5 COMPARISON OF CONTAMINANT DIFFUSION FIELDS BY MEANS OF SVE1, 2, 3

(1) Study Based on SVE1

The values of SVE1 for all cases and for all contaminant generation points are given as the upper line in each space in Table 6. SVE1 shows larger value when the contaminant is generated near the wall.

(2) Study based on SVE2

The values of SVE2 are tabulated as the lower line in each space in Table 6. SVE2 shows smaller value when the contaminant is generated near the wall. It increases as the source point moves towards the center of the room.

(3) Study based on SVE3

A high value for SVE3 appears near the ceiling for all cases. When a recirculating flow is formed around the obstacle, SVE3 becomes higher in that region. The supplied clean air takes longer way to reach these areas, so there is much greater possibility that the air in this region will be contaminated.

15. CONCLUSIONS

It is confirmed that numerical simulation of the velocity and diffusion fields in a room is very useful in comprehending flow and diffusion patterns. The characteristics of the airflow and contaminant diffusion in a room with ceiling supply openings are summed up as follows.

(1) Mean flow structures of the airflow are modeled very well as serial combinations of flow units, which consist of one supply jet and the rising streams around it.

(2) The resulting diffusion field is mainly caused by the convection of the mean airflow. The structure of the diffusion fields also becomes very clear by introducing the concept of flow units.

(3) The supply openings have great influence on the flow fields and also a rather large influence on contaminant diffusion fields. When the numbers of the supply openings are decreased, the flow units corresponding to the eliminated supply openings disappear and the remaining flow units expand.

(4) The significant effect of the placement of an obstacle on the flow field is usually confined within the space around the obstacle. But the flowfield within the 'flow units' in which the obstacle exists is influenced greatly.

(5) Even if the effect of the placement of an obstacle on the velocity field seems to be small, the contaminant diffusion field is often influenced greatly by the arrangement of a flow obstacle.

(6) The table-type flow obstacle is generally superior to the box-type flow obstacle from the view point of ventilation efficiency.

(7) The new scales of ventilation efficiency, which are the spatial average concentration (SVE1), the mean radius of diffusion (SVE2), and the concentration in case of contaminant generated uniformly throughout a room (SVE3), are very useful measures for comparing the different diffusion fields and for quantitatively comprehending diffusion properties. These scales are strong tools that summarize in clear fashion very complex information on room diffusion fields, which is hard to characterize clearly by any other means.

Table 6. Values of SVE1 and SVE2 (Case 0 without obstacle and Case 1~4 with obstacle)

sources / Case No.	near the wall (point A)	under supply jet (point B)	between supply jets (point D)	center of the room (point E)
Case 0 (without obstacle)	1.7 *¹ / 3.1 *²	1.3 / 3.2	1.5 / 3.6	1.4 / 4.2
Case 1	2.1 / 2.5	—	—	1.6 / 4.3
Case 2	—	1.9 / 3.7	—	1.6 / 4.2
Case 3	—	—	1.7 / 3.2	1.5 / 4.0
Case 4	1.4 / 2.5	—	—	1.3 / 4.2

*¹ upper line of the space : SVE1 (non-dimensionalized by Co)
*² lower line of the space : SVE2 (non-dimensionalized by Lo)

REFERENCES

Chieng, C.C., and Launder, B.E. 1980. "On the calculation of turbulent heat transport downstream from an abrupt pipe expansion." Numerical Heat Transfer,Vol.3,pp.189-207.

Kato, S., and Murakami, S. 1988a. "New ventilation efficiency scales based on spatial distribution of contaminant concentration aided by numerical simulation." ASHRAE Transactions,Vol.94,Part 2,pp.309-330

Kato, S.; Murakami, S.; and Nagano, S. 1988b. "Study on diagnostic system for simulation of turbulent flow in room(Part 17). Investigation on each type wall boundary of k-ε 2-equation model(No.1)." Transactions of annual meeting of SHASEJ,pp.573-576.

Lauder, B.E.,and Spalding, D.B. 1974. "The numerical computation of turbulent flows." Computer Methods in Applied Mechanics and Engineering, Vol.3,pp.269-289.

Murakami, S., and H, Komine. 1980. "Measurement of three components of turbulent flow with tandem hot-wire probe." Transactions of Architectural Institute of Japan, No.297, pp.59-69.

Murakami, S.; Kato, S.; and Suyama, Y. 1987. "Three-dimensional numerical simulation of turbulent airflow in a ventilated room by means of a two-equation model." ASHRAE Transactions, Vol.93,Part2,pp.621-642.

Murakami, S.; Kato, S.; and Suyama, Y. 1988. "Numerical and experimental study on turbulent diffusion fields in conventional flow type clean rooms." ASHRAE Transactions, Vol.94,Part2,pp.469-493.

Murakami, S.; S. Kato, and Y. Suyama, 1989 "Numerical study on diffusion field as affected by arrangement of supply and exhaust openings in conventional flow type clean room," ASHRAE Transactions, Vol.95, Part 2.

Murakami, S.; S. Kato, and Y. Suyama, 1990. "Numerical study on flow an d contaminant diffusion field as affected by flow obstacles in conventiona l flow type clean room." ASHRAE Transactions, Vol.96,Part 2.

Nagano, S.; Murakami, S.; and Kato, S. 1988. "Study on diagnostic system for simulation of turbulent flow in room(Part 18). Investigation on each type wall boundary of K-ε 2-equation model(No.2)." Transactions of annual meeting of SHASEJ,pp.577-580.

Rodi, W. 1984. "Turbulence models and their application in hydraulics." IAHR. The Netherlands.

Discussion

Paper 32

J.Van Der Maas (LESO-EPFL, Switzerland)

You have shown that CFD allows the calculation of forced flows. Which developments do you foresee for mixed convection? Which problems do you think will remain unsolvable for a long time?

S.Muracami (Tokyo, Japan)

We have finished the simulation of the flowfield of mixed connection by means of the K-e model with certain accuracy. Furthermore, we have achieved the simulation of the same flowfield by means of Algebraic-stress model with higher accuracy. These results will be reported in the forthcoming AIVC Conference and ASHRAE meeting, etc.

J.Axley (MIT, USA)

In spite of impressive analytical capabilities proved by CFD we must recognise that CFD analysis has the major limitation that it presently can be applied to the analysis of flow regimes of relatively simple geometries (e.g. more or less single rooms) - driven by relatively simple boundary conditions (e.g., steady boundary conditions). CFD analysis will not be able to be applied to whole building simulation for some time.

S.Muracami (Tokyo, Japan)

Yes, CFD has many difficulties in its application now. But its history in this field is only 10 years or so. Since the development of CFD method and the super-computer is rapid, the successful applications of CFD into the ventilation problems are increasing rapidly. Its future seems to be very promising. But, as you say, it will take some time for the application of simulation to whole building. The concept of a micro-macro mixed model is very helpful to overcome such type of difficulties. The treatment of complex boundary can be solved by the technique of composite grid adaptive grid, BFC, FEM, etc. The simulation of unsteady flowfield has become rather easy by the development of Large Eddy Simulation.